West Maui Watershed Study

West Maui, Hawaii

Draft Report
1 June 2021

Prepared by:

U.S. Army Corps of Engineers, Honolulu District

Prepared for:

State of Hawaii, Department of Land and Natural Resources

APPENDIX 1

HYDROLOGY AND HYDRAULICS

This page is intentionally blank.

EXECUTIVE SUMMARY

The final event-based sediment load and distribution time series data at the outlet of five key watersheds within the study area were determined by flood frequency analysis, use of hydraulic modeling, calibration of event-based sediment loads to previous investigations, and analysis of the trap efficiency of existing detention basins. The five watersheds selected for this type of analysis were Wahikuli, Honokowai, Kahana, Kaopala, and Honolua. Peak flow estimates were developed for all eleven watersheds within the study area: Wahikuli, Hanakaoo, Honokowai, Mahinahina, Kahana, Kaopala, Honokeana, Napili 4-5, Napili 2-3, Honokohua, and Honolua.

The flood frequency analysis included stream gage analysis, application of regional regression equations, and development of a rainfall-runoff model using HEC-HMS software. The rainfall-runoff model was initially calibrated to replicate specific historical storms; however, the limited number of sites and storm events that could be used for calibration proved this method to be ineffectual. However, a Bulletin 17C stream gage analysis on two sites in the Honokohau and Honokowai watershed provided a strong level of confidence based on long periods of record and the rainfall-runoff model was calibrated to match these results. The final peak flow estimates adopted by this study are presented in Section 5.4.

The output of the calibrated rainfall-runoff model was used as input for the two-dimensional, unsteady flow hydraulic model that was developed using HEC-RAS software. Models were created that are representative of the lower reaches within the Wahikuli, Honokowai, Kahana, Kaopala, and Honolua watersheds. Flow and shear stress time series data (outputs from the hydraulic model) were then used to develop time series data representative of the likely sediment load within the reach and at the outlet.

The sediment load time series data was developed using the *excess shear* equation, in addition to relying upon previous conclusions drawn by USGS regarding the annual sediment load for each watershed, the types of event that trigger a sediment plume at the outlet, and data collected in the field throughout the study.

The effectiveness of the existing detention basins at Kaopala, Kahana, and Honokowai were determined by using Camp's settling velocity equations. The sediment

load time series data was then adjusted to determine the probable sediment load that was released into the ocean based on existing site conditions. These results are presented in Section 7.2. The level of accuracy of these results is commensurate with the level of data that was available during this study.

TABLE OF CONTENTS

LIST OF ACRONYMS & ABBREVIATIONS

CWRM	Commission on Water Resource Management
DAR	Division of Aquatic Resources
DLNR	Department of Land and Natural Resources
HEC	Hydrologic Engineering Center
HMS	Hydrologic Modeling Software
LMSL	Local Mean Sea Level
NOAA	National Oceanic and Atmospheric Administration
RAS	River Analysis Software
State	State of Hawaii
USGS	U.S. Geological Survey

This page is intentionally blank.

1 Introduction

1.1 Authority

The authority for the West Maui Watershed Study is provided by Section 729 of the Flood Control Act of 1996, in accordance with the policies and procedures prescribed by the Chief of Engineers.

1.2 Project Sponsor

The non-federal sponsor for the West Maui Watershed Study is the State of Hawaii (State), Department of Land and Natural Resources (DLNR).

1.3 Study Area

The study area encompasses a collection of about eleven adjacent watersheds (Figure 1-1) on the leeward side of the West Maui Mountains, north of the town of Lahaina, Maui. These watersheds are grouped by the State of Hawaii into five surface water hydrologic units: Wahikuli (6009[1]), Honokowai (6010), Kahana (6011), Honokahua (6012), and Honolua (6013).

1.4 Purpose

The intent of the West Maui Watershed Study is to contribute to the restoration, enhancement and resiliency of West Maui coral reefs and nearshore waters through the reduction of land-based pollution threats. Several alternatives that have potential to reduce the amount of terrestrial sediment being discharged into the marine environment will be proposed and evaluated as part of this study. The results of this study will be shared with key stakeholders and local decision-makers to provide them with additional information to rely upon in the future.

[1] Each surface water hydrologic unit has a unique 4-digit code assigned by the State's Commission on Water Resource Management.

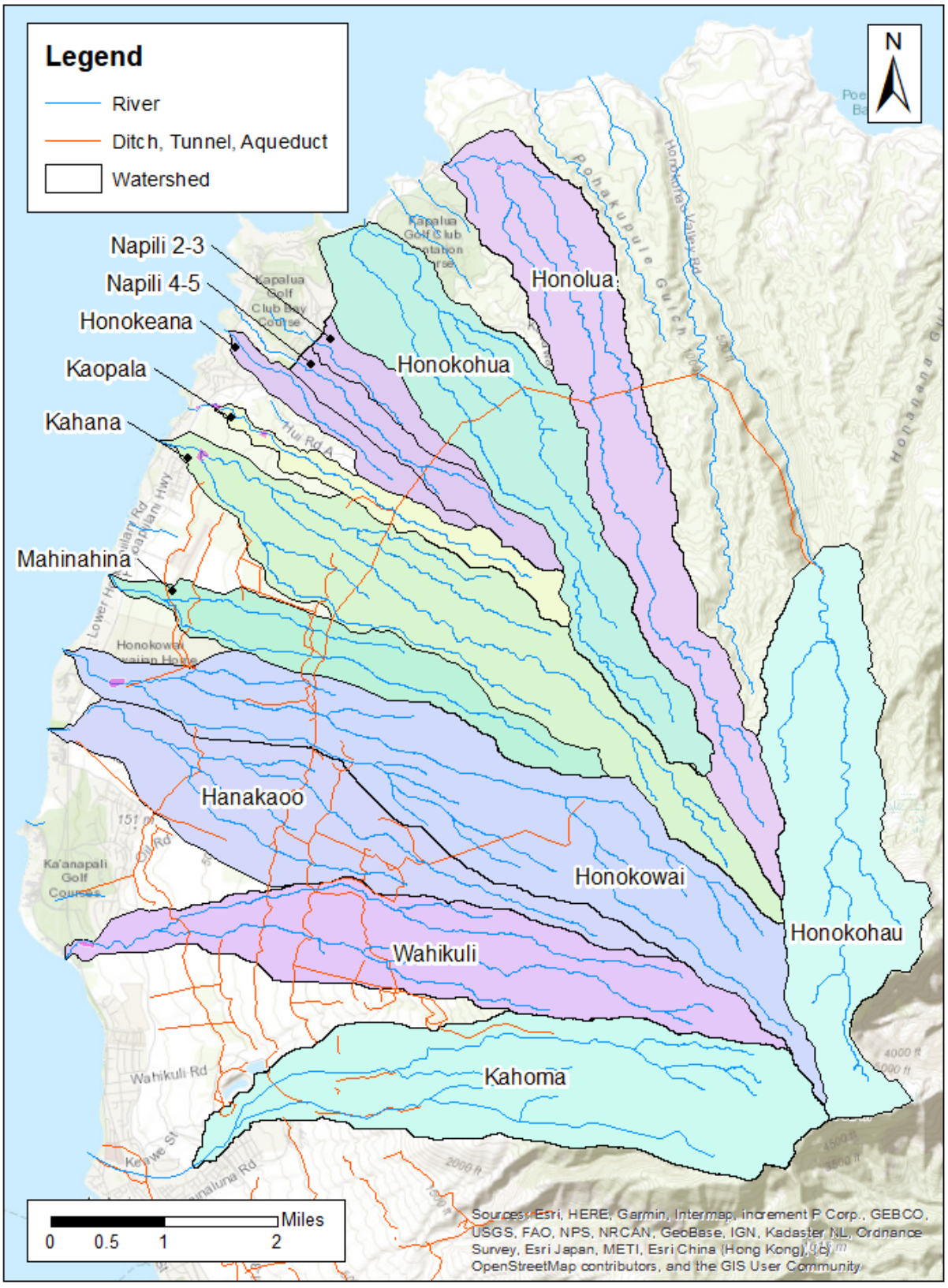

Figure 1-1: Watershed Map, West Maui, Hawaii

1.5 Previous Investigations and Reports

A list of previous work completed by the U.S. Army Corps of Engineers (USACE) and others is provided below, including a summary of key findings directly relevant to this study:

- *Wahikuli-Honokowai Watershed Management Plan*, *Volume 1: Watershed Characterization* (National Oceanic and Atmospheric Administration, Coral Reef Conservation Program, 2012).
- *Wahikuli-Honokowai Watershed Management Plan*, *Volume 2: Strategies and Implementation* (Coral Reef Conservation Program, 2012).
- *Low-Flow Characteristics of Streams in the Lahaina District, West Maui, Hawaii.* Scientific Investigations Report 2014-5087, (U.S. Department of the Interior, U.S. Geological Survey [USGS], 2014).
- *Spatially Distributed Groundwater Recharge Estimated Using a Water-Budget Model. for the Island of Maui, Hawai'i, 1978-2007.* Scientific Investigations Report 2014-5168, (USGS, 2014).
- *Reconnaissance Sediment Budget for Selected Watersheds of West Maui, Hawai'i.* Open-File Report 2015-1190. (USGS, 2015).
    - Streambank erosion of historic terraces of sands, silts, and clays, are likely the primary source of sediment in the channel system, resulting in annual plume generation in the nearshore waters of West Maui, Hawaii.
    - Treatments of former agricultural fields, roads, and reserve forests are not likely to measurably affect sediment pollution from smaller, more frequent storms.
    - As a reconnaissance budget, erosion-rate estimates were based on work elsewhere in the Hawaiian Islands and have great uncertainties.
- *West Maui Watershed Plan: Kahana, Honokahua and Honolua Watersheds, Characterization Report* (USACE and DLNR, 2016).
- *West Maui Watershed Plan: Kahana, Honokahua and Honolua Watersheds, Strategies and Implementation Report* (USACE and DLNR, 2016).

- *West Maui Wahikuli & Honokowai Priority Watershed Area, Reef Condition Report* (DAR, 2016).
- *Sediment Budget for Watersheds of West Maui, Hawaii*. Scientific Investigation Report 2019-xxxx. (USGS, 2019).
    - Coastal sediment plumes occur at least 3-5 times per year in source watersheds.
        - Although total rainfall has decreased since the 1970s, more of it now occurs during short, intense storms capable of causing runoff and erosion.
    - Historic fill terraces (the primary source of sediment) are found only downstream of historic agricultural fields, and are composed of silt and fine sand.
    - Several field experiments were conducted, including a survey of historic fill terraces, the installation and periodic monitoring of erosion pins, and cohesive strength meter (CSM) testing, which are described in Section 4.3.
    - Bank erosion of fill terraces from a few watersheds likely dominates the current annual fine sediment load to the nearshore, with Kahana producing the largest annual input of 285 metric tons, the equivalent of 29 dump-truck loads every year.
    - The storms capable of generating widespread runoff from agricultural fields are decadal events.
- *Instream Flow Standard Assessment Report, Island of Maui, Hydrologic Unit 6010, Honokowai*. Draft PR-2019-01. (CWRM, 2019)
- *Instream Flow Standard Assessment Report, Island of Maui, Hydrologic Unit 6013, Honolua*. Draft PR-2019-02. (CWRM, 2019)
- *Instream Flow Standard Assessment Report, Island of Maui, Hydrologic Unit 6014, Honokohau*. Draft PR-2019-03. (CWRM, 2019)

1.5.1 **USACE Committee on River Engineering**

In August 2019, the USACE Committee on River Engineering (CRE) visited several sites in West Maui to provide recommendations on effective management strategies for reducing in-stream erosion, technical modeling, and next steps in the planning process. Their recommendations include the following:

- Develop a Water Budget using HEC-HMS, identifying sources of water supply and diversion.
- Verify the Sediment Budget developed by USGS; verify the assumption that sediment is primarily sourced from in-stream erosion versus overland sources.
- A sediment model analyzing trap efficiency would be helpful in evaluating the effectiveness of the alternatives currently proposed. The existing field data available does not support detailed erosion modeling (e.g. BSTEM, MUSLE).
- Determine the sediment tolerance of the reefs; understand the types and amounts of sediment that the reefs can tolerate by either conducting a thorough literature search on this subject or working with local experts to develop this information.

There were several different approaches considered by CRE to address in-stream erosion: 1) stabilizing the problematic banks, 2) removing the erosive bank material directly, 3) capturing the sediment with an in-stream feature, 4) diverting all or some portion of the flow to a side-channel feature (e.g. offset stilling basin), 5) altering the flow regime (reducing the amount of flow in the channel with an upstream feature), and 6) flocculation. Generally, capturing the sediment with an in-stream feature or diverting flow to a side-channel feature seemed to be the most promising. Removal of the erosive bank material, altering the flow regime, and flocculation were not recommended.

- At Honolua, one alternative was considered that included lowering the floodplain and arranging boulders at constrictions to generate floodplain residence time to encourage sediment settlement. For this type of alternative, a two-dimensional (2D) hydraulic model would be useful in computing a change in velocity field and residence time.

- In Wahikuli, two sediment stilling basin site proposals were considered. A simple sediment model could investigate the value of different configurations.

2 Watershed Description

2.1 Location

The entire study area is approximately 36 square miles (mi^2) and encompasses a collection of eleven adjacent watersheds (Figure 1-1) on the leeward side of the West Maui Mountains, north of the town of Lahaina, Maui. These eleven watersheds have been identified as Wahikuli, Hanakaoo, Honokowai, Mahinahina, Kahana, Kaopala, Honokeana, Napili 4-5, Napili 2-3, Honokohua, and Honolua. The adjacent watershed of Honokohau was also included in this study as it provides a long record of continuous streamflow data (streamflow data within the study area itself is very limited).

The State of Hawaii's classification system groups these individual watersheds into just five surface water hydrologic units: Wahikuli (6009[2]), Honokowai (6010), Kahana (6011), Honokahua (6012), and Honolua (6013).

2.2 Topography

The summit of Pu'u Kukui is the highest point in the study area at 5,785 feet above mean sea level (ft MSL). Basin lengths range from 3.6 miles (mi) for Kaopala to 8.2 mi for Honokowai. The steep river profile originating in the mountains results in each basin having an oblong shape as water travels west-northwest toward the Pacific Ocean with limited meandering. Honokowai is the steepest basin, with an average basin slope of about 53 percent (%). Wahikuli, Kahana, Honokohua, and Honolua are also steep with an average basin slope between 40-50%. The smaller watersheds that originate at a lower elevation (e.g. Hanakaoo, Mahinahina, Kaopala, Honokeana, and Napili) have an average basin slope between 15-30%.

2.3 Geology and Soils

The West Maui Mountains were formed through at least three series of major volcanic eruptions during its shield building period: the Wailuku volcanic series, the Honolua volcanic series, and the Lahaina volcanic series. Following the cessation of West Maui volcanism 500,000 years ago, the rapid erosion and valley incision of West Maui

[2] Each surface water hydrologic unit has a unique 4-digit code assigned by the State's Commission on Water Resource Management.

has produced broad alluvial fans with unconsolidated dunes of lithified to semi-lithified calcareous sand on the western slopes.

2.4 Climate

Hawaii has a subtropical climate with temperatures that are mild and fairly uniform throughout the year. The mean annual temperature at Kahului, near Wailuku, is 73.2° Fahrenheit (F), with an average maximum of 81.9°F and average minimum of 64.5°F (Honolulu Weather Forecast Office, 2020). The

The climate of the Hawaiian Islands is characterized by a two-season year; a 5-month summer or dry season and a 7-month winter or wet season; mild and uniform temperatures, strikingly marked geographic differences in rainfall, generally humid conditions, and prevailing dominance of trade wind flow from the northeast. During the 5-month summer from May through September, trade winds prevail 80-95 percent of the time. During the 7-month winter from October through April, the prevalence of the trade winds decreases to 50-80 percent. Although the northeasterly trade winds produce most of the annual rainfall over the Hawaiian Islands, it is during the absence of these winds that the flood producing rainfall occurs. In particular, southerly winds bring moist warm air that creates “Kona” storms which produce the damaging floods in Hawaii. These storms usually occur during the winter months. The climate of the West Maui watersheds is tropical with cooler and wetter areas at higher elevations in the belt of the northeasterly trade winds. The average monthly precipitation ranges from 3.35 inches in the wettest month (December) to 0.2 inches in the driest month (June) (U.S. Climate Data, 2017).

2.5 Dams and Reservoirs

As part of the Honolua Watershed Project, sponsored by the West Maui Soil and Water Conservation Districts (SWCD) and the County of Maui, eight desilting basins were constructed within the West Maui study area.

2.5.1 **Napili 2-3 Basin**

National Dam ID: HI00128 State Dam ID: MA-0128

Location: 20°59'38.31"N, 156°39'44.49"W

The Napili 2-3 Basin, "Structure #1," was constructed in 1988 and is currently maintained by the County of Maui, Department of Public Works (DPW). The basin has been adapted to serve as a golf course water feature. It is operated to retain water at all times and has not been dredged for several years. There are indications that sediment/silt deposition is 8 feet thick near the outlet, tapering to 1.5 feet thick at the inlet. Discharges from Napili 2-3 consistently break into Napili Bay two hours before any discharge occurs from Napili 4-5, presumably because there is less active storage volume in the Napili 2-3 basin (NRCS, 2011).

Source: State of Hawaii, DLNR, Dam Inventory System

Photo 2-1: Aerial photo of the Napili 2-3 basin

2.5.2 **Napili 4-5 Basin**

National Dam ID: HI00127 State Dam ID: MA-0127

Location: 20°59'32.56"N, 156°39'55.09"W

The Napili 4-5 Basin, "Structure #2," was constructed in 1985 for watershed protection (reduction of sediment and debris transport) and flood prevention. The basin is owned by the County of Maui, who has designated its Department of Public Works as the agency responsible for maintenance.

The basin was modified in 2011, with funding from the Napili Bay and Beach Foundation, to include a tri-level outlet valve for flow management and a grassed waterway to slow and filter runoff released from the outlet. During small storm events the valve can be set to allow longer retention time, which allows more sediment to settle out of the water column and prevent sediments from being discharged into nearshore waters. During larger storm events the valve can be adjusted and water can pass through. Since this modification, there has reportedly been no visible plumes near the outlet with the exception of the runoff caused by Hurricane Olivia in September 2018 (Napili Bay and Beach Foundation). The Napili 4-5 dam is being considered for removal from the State Dam Safety Program because of its small size.

Source: State of Hawaii, DLNR, Dam Inventory System

Photo 2-2: Aerial photo of the Napili 4-5 basin

2.5.3 **Honokeana Basin**

Location: 20°59'24.60"N, 156°40'1.11"W

Honokeana Basin, "Structure #3," was constructed in 1997 for watershed protection (reduction of sediment and debris transport) and flood prevention. It is not regulated by the DLNR Dam Safety Program. The basin is owned by the County of Maui, who has designated its Department of Public Works as the agency responsible for maintenance. This basin has acceptable functioning to reduce sediment transport to nearshore waters as it is appropriately sized for its drainage area. Below the outlet, water is causing erosion adjacent to Lower Honoapi'ilani Road.

Source: Google Earth

Photo 2-3: Aerial photo of the Honokeana Basin

2.5.4 **Kaopala Basin**

National Dam ID: HI00134 State Dam ID: MA-0134

Location: 20°58'55.22"N, 156°40'13.45"W

The Kaopala Basin, "Structure #4," was constructed in 1998 for watershed protection (reduction of sediment and debris transport) and flood prevention. The basin is owned by the County of Maui, who has designated its Department of Public Works as the agency responsible for maintenance. This basin is considered undersized and is constrained by site topography. The open outlet (Photo 2-5), located near the bottom of the reservoir basin, allows for sediment-laden water to pass through easily.

In September 2014, the University of Hawaii at Manoa, Water Resources Research Center collected sediment samples from Kaopala Basin as part of an *Engineering Analysis and Development of Retrofit Designs for Sediment Retention at Honokowai Structure #8*. The sample showed a relatively high percentage of gravel (23%), sand (57%) and much smaller amounts of silt and clay (20%). The composition may reflect gravel contributions from ridge activities or perhaps only the large sediments are settling out of the water.

Photo 2-4: Looking upstream at Kaopala Basin

Source: State of Hawaii, DLNR, Dam Inventory System

Photo 2-5: Upstream end of outlet intake, Kaopala Basin

Photo 2-6: Looking downstream at Kaopala Basin

2.5.5 **Kahana Basin**

National Dam ID: HI00126

State Dam ID: MA-0126

Location: 20°58'32.50"N, 156°40'19.04"W

The Kahana Basin, “Structure #5,” was constructed in 1984 for watershed protection (reduction of sediment and debris transport) and flood prevention. It has a 50 feet high earthen dam and a maximum storage capacity of 73 million gallons. The basin outlet consists of a concrete structure with ports for trapping coarse debris. An emergency spillway south of the dam conveys water from high flow storm events to prevent overtopping of the earthen dam structure. The basin is considered undersized for its drainage area.

The basin is owned by the County of Maui, who has designated its Department of Public Works as the agency responsible for maintenance. Buried outlet pipes have prevented complete drying of the basin, which in turn prevents equipment from being able to remove sediments and results in significantly decreased retention volume.

Photo 2-7: Looking upstream at Kahana Basin

2.5.6 **Pohakuka‘anapali Basin**

Location: 20°57'57.64"N, 156°40'42.65"W

Pohakuka‘anapali Gulch is a small watershed located between the larger Kahana and Mahinahina watersheds. It empties a drainage area of approximately 0.6 mi^2 into the ocean south of Pohaku Park. Upstream of Honoapiilani Hwy, there is an earthen embankment dam similar in design to the Mahinahina Dam: the Pohakuka‘anapali Basin, “Structure #5.” This impoundment is maintained by the County and is not regulated by the DLNR Dam Safety Program. Pohakuka‘anapali Gulch is not one of the primary watersheds being evaluated under this study.

2.5.7 **Mahinahina Basin**

Location: 20°57'29.54"N, 156°40'51.61"W

Mahinahina Basin, "Structure #7" (Photo 2-8) was constructed in 1995 as part of the larger Honolua Watershed Project. It is owned by the County of Maui, who has designated its Department of Public Works (DPW) as the agency responsible for maintenance. It is not regulated by the State Dam Safety Program. The basin is effective at trapping fine sediments due to a long retention time and the orifice sizing of the outlet. The dam was also designed to overtop during large storm events, as evidenced by the reinforced concrete dam face at the downstream side of the structure.

DPW mows the basin approximately once or twice per month. Sediment typically accumulates within the basin in the area of the concrete embankment and is removed with a backhoe and loader approximately two or three times per year. The sediment level typically ranges between 1.5 to 2 feet at the time of removal, but does not exceed 3 feet due to regular maintenance. An estimated 250 – 500 cubic yards (CY) of sediment is removed annually (this is roughly equivalent to a 6 inch deep layer of sediment covering between 13,500 – 27,000 square feet [ft^2] of land area). To alleviate berm erosion and subsequent sediment deposition that had been occurring on the perforated drainage pipe, a riprap wall was constructed around the pipe.

Photo 2-8: Mahinahina Basin, Looking northeast from the top of the embankment

Photo 2-9: Mahinahina Basin, inlet pipe

Photo 2-10: Mahinahina Basin, twin culverts under Honoapiilani Hwy

2.5.8 **Honokowai Basin**

National Dam ID: HI00130

State Dam ID: MA-0130

Location: 20°56'46.78"N, 156°41'0.50"W

Honokowai Dam, Structure #8, is located in the Honokowai watershed, approximately 2,600 ft from the Honokowai shoreline. The facility is owned by the County of Maui, who has designated its Department of Public Works (DPW) as the agency responsible for maintenance. It was constructed in 1995 with the primary objective of reducing the sediment load transported to the ocean. The basin was sized for trap efficiency and not for sediment volume over a period of time (requiring periodic removal of the sediment after each major storm event).

The basin outlet consists of a concrete structure with ports for trapping coarse debris cast incrementally in height along one side of the structure and larger overflow ports at the top of the structure that discharge into the principal outlet channel. An emergency spillway south of the dam conveys water at high flow storm events to prevent overtopping of the earthen dam structure.

DPW mows the basin and berm area on an as needed basis, with more mowing necessary during the winter months. Debris is removed from the concrete outlet structure an average of three times per year depending on the frequency of debris deposition form large storm events. Debris has been observed as mostly large, woody, and vegetative, as opposed to fine or coarse sediment. The water level has not been observed overtopping the dam, and debris has been observed on top of the concrete outlet structure approximately six times over a period of 20 years.

Photo 2-11: Aerial photograph of Honokowai Dam Structure #8

Photo 2-12: Honokowai Intake Structure

3 Geographic Information Systems Data

3.1 Datum and Projection

The datum and projection for this study is as follows:

Horizontal projection: State Plane Zone 2 (US Survey Feet)

Horizontal datum: NAD83 (PA11)

Vertical Datum for Land Applications: Local Tidal Datum – MSL

Tidal Epoch: 1983 – 2001

Geoid: 2012B

3.2 Elevation

The following sources of elevation data were used in this study:

Table 3-1: Elevation Data Type and Sources

Survey year	Agency	Data type	Location
2005 - 2013	State of Hawaii	DTM	about 1.0 mi inland from coast
2013	USGS	DEM	United States

Light Detection and Ranging (LiDAR) data were provided by an online GIS database under the Hawaii Statewide GIS Program. This database reflects a multi-agency effort to establish and promote the use of GIS technology in Hawaii State Government, led by the State of Hawaii, Office of Planning. A digital terrain model (DTM) was available to download, based on LIDAR collected by various agencies between 2005 and 2013 along the coast of West Maui.

Areas within the study area that were not covered by LIDAR were supplemented using an elevation raster from the USGS National Elevation Dataset (NED). The NED was developed by merging the highest resolution, best quality Digital Elevation Model (DEM) data available across the United States into a seamless raster format. Across the study area, digital elevation data was available at resolutions of 1/3 arc-second (approx. 10 meters). These data are distributed in geographic coordinates in units of decimal degrees, and in conformance with NAD83 (USGS).

3.3 Imagery

High resolution imagery used for background mapping of the study area is from DigitalGlobe, the National Geospatial-Intelligence Agency and the USGS. World Imagery, provided by Esri, was used for larger scale background mapping, such as when it was necessary to show the entire island of Guam.

3.4 Basin, subbasin and river delineation

GIS data were used to delineate the basins (Table 5-13), subbasins (Table 5-14) and rivers. Each basin was divided into subbasins based on key locations in the watershed (e.g. the location of a streamflow gage, junction, or existing detention basin).

Table 3-2: Basin identification and information

Basin ID	Basin name	Drainage area (mi^2)	Centroid location	
			Latitude	Longitude
1	Wahikuli	3.89	20.911475	-156.639656
2	Hanakaoo	3.37	20.928895	-156.657939
3	Honokowai	5.80	20.929811	-156.632436
4	Mahinahina	1.80	20.948749	-156.650262
5	Kahana	4.35	20.952354	-156.635833
6	Kaopala	0.812	20.967475	-156.642701
7A	Honokeana	0.554	20.978622	-156.652712
7B	Napili 4-5	0.814	20.974488	-156.640926
7C	Napili 2-3	0.433	20.983515	-156.646616
8	Honokohua	4.13	20.975677	-156.629628
10	Honolua	4.28	20.976841	-156.615055
12	Honokohau	4.32	20.927803	-156.585456

Table 3-3: Subbasin identification and information

Subbasin ID	Basin name	Drainage area (mi^2)	Centroid location	
			Latitude	Longitude
1A	Wahikuli	0.237	20.914075	-156.68211
1B	Wahikuli	2.28	20.909011	-156.635398
1C	Wahikuli	1.37	20.915133	-156.639399
2A	Hanakaoo	0.679	20.929989	-156.673387
2B	Hanakaoo	2.69	20.928619	-156.654040
3A	Honokowai	0.243	20.947352	-156.683530
3B	Honokowai	1.56	20.930424	-156.641111
3C	Honokowai	1.77	20.941118	-156.650151
3D	Honokowai	2.23	20.918459	-156.606669
4A	Mahinahina	1.80	20.948749	-156.650262
5A	Kahana	0.060	20.97671	-156.673711
5B	Kahana	1.36	20.956836	-156.648874
5C	Kahana	2.92	20.949757	-156.628927
6A	Kaopala	0.812	20.967475	-156.642701
7A	Honokeana	0.554	20.978622	-156.652712
7B	Napili 4-5	0.814	20.974488	-156.640926
7C	Napili 2-3	0.433	20.983515	-156.646616
8A	Honokohua	2.60	20.971047	-156.629524
8B	Honokohua	1.53	20.983527	-156.629806
10A	Honolua	0.386	21.008828	-156.632857
10B	Honolua	2.78	20.965825	-156.611664
10C	Honolua	1.11	20.993317	-156.617362
12A	Honokohau	4.32	20.927803	-156.585456

3.5 Land Cover and Land Use

A general land cover and land use raster was developed by OCM in 2005 based upon high resolution (1 to 5 meter) aerial and satellite imagery. This raster was used to compute the directly connected impervious areas for the rainfall-runoff model (Section 5.3.2). A detailed land cover raster was also developed in 2010 by OCM, but was not used in this study.

A detailed land cover raster was also provided by the Pacific Regional Integrated Sciences and Assessments (PAC-RISA) program, which provides land cover data representative of 2017 conditions and "future" land cover for four different scenarios: 1) a conservation-focused future, 2) a status-quo future, 3) a development-focused future, and 4) a future in which high native forest restoration and high urban development coexist. When comparing the "existing" 2017 land cover with "future" scenario 2 (status-quo), the change in land cover is not significant with the exception of the extensive fallow agricultural lands becoming slightly grassed. There is also a reduction in agricultural lands in the lower Hanakaoo watershed, and a slight increase in agricultural lands in the lower Honokowai lands (Brewington, 2018). The "existing" land cover raster, representative of 2017 conditions, was used to create the Manning's n layer in the hydraulic model (Section 6.2.3).

3.6 Soil Data

A water permeability shapefile provided by the Hawaii Soil Data Atlas was used to determine initial loss rates for the hydrologic model, as described in Section 5.3.2 (University of Hawai'i, 2014). A soil classification survey raster was provided by the NRCS's Web Soil Survey (NRCS) and used to determine initial loss and transform parameters for the hydrologic model.

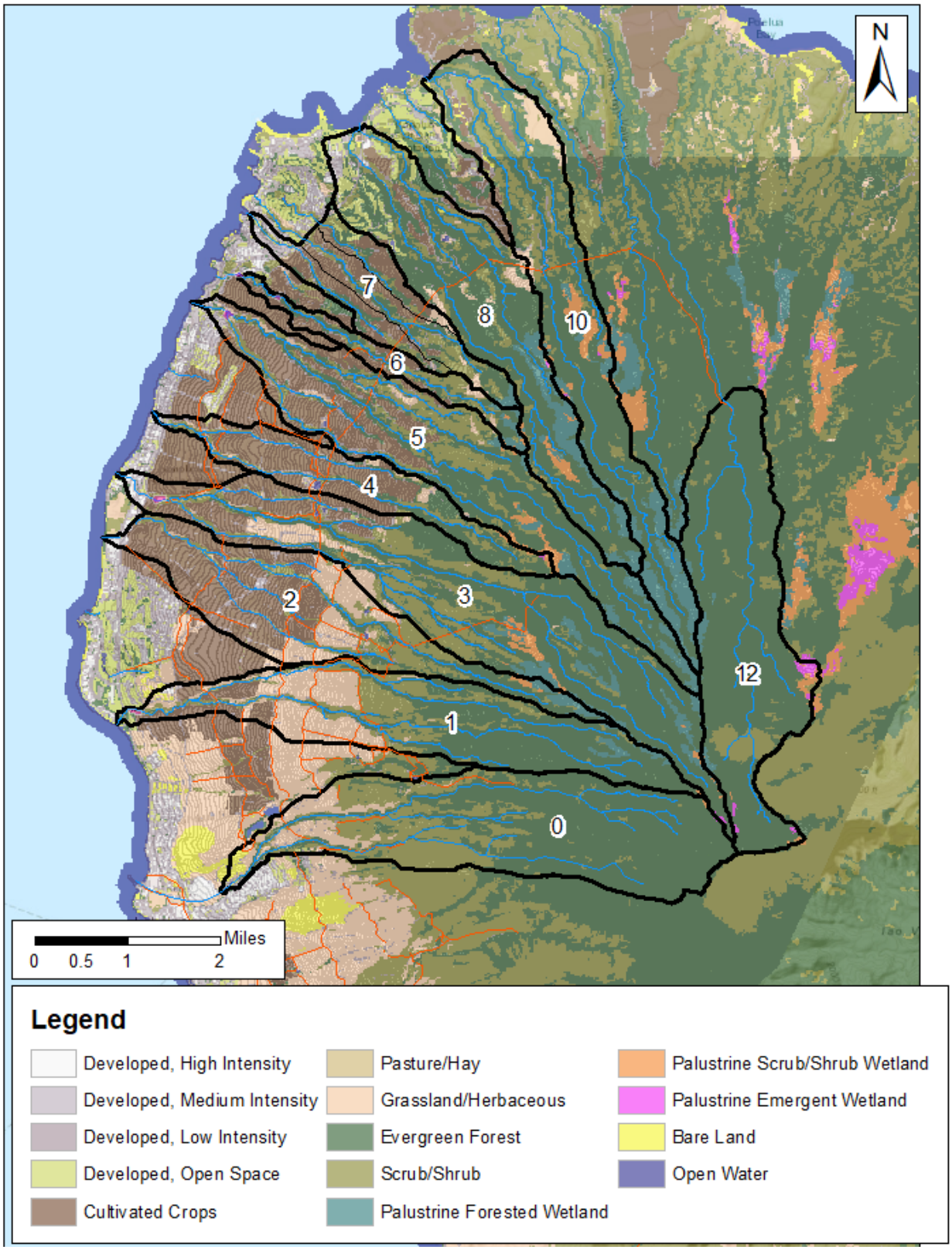

Figure 3-1: Land Cover Types in West Maui, Hawaii (OCM, 2005)

4 Data Collection

This section describes available climate, stream, and sediment data within the study area and the adjacent watersheds of Kahoma and Honokohau. Due to the limited availability of streamflow records within the study area, the adjacent watersheds of Kahoma and Honokohau were also included in the hydrologic analysis for comparative purposes.

4.1 Climate

Climate data (e.g. rainfall) was available at one USGS and four National Oceanic and Atmospheric Administration (NOAA) rain gages within or near the study area (NCEI). There are also four other rainfall stations located within the study area that are monitored by West Maui Ridge to Reef (R2R). These gages are listed in Table 4-1 and each provide instantaneous data in either 5 or 15-minute intervals. Historical, instantaneous data were used to calibrate the hydrologic model (see Section 5.3.4).

Point precipitation data for annual exceedance rainfall was obtained from the National Weather Service's (NWS) NOAA Atlas 14 Precipitation-Frequency Data Server (PFDS). This source presents rainfall frequencies from recurrence intervals of 1 to 500 years (100% to 0.2% AEP) at various locations across the study area (NWS, 2014). The location points used to extract PFDS data were the approximate centroid locations for each subbasin (Table 5-14). This data was put into the calibrated hydrologic model to compute the peak flow estimates for various recurrence intervals.

Table 4-1: Climate Station Inventory

Agency	Site Number / Network:ID	Site Name	Period of Record	Datum of gage (ft above LMSL[1])	Latitude	Longitude
USGS	2053271 56351102	380.0 Puu Kukui Rain Gage at alt 5,771 ft, Maui, HI	2005 – 2020	5,771	20.89083	-156.58638
NOAA	COOP:510530	Field 28 Reservoir 474.2, HI US	2006 – 2014	1,157	20.96722	-156.63750
NOAA	COOP:510541	Field 46 474, HI US	1978 – 2005	1,050	20.98888	-156.62750
NOAA	COOP:518407	Puukolii 457.1, HI US	2002 – 2014	421	20.92861	-156.67361
NOAA	COOP:515177	Lahaina 361, HI US	1977 – 2001	11.6	20.8788	-156.6741
West Maui R2R	--	Upper Honokowai	2016 –2020	2,951	20.92333	-156.62083
West Maui R2R	--	Maui Cultural Lands Honokowai	2016 – 2020	900	20.93750	-156.65222
West Maui R2R	--	Kaanapali Shores	2016 –2018	19.6	20.94305	-156.68694
West Maui R2R	--	Honokowai Lower	2016 –2020	2,602	20.92527	-156.62583

[1]: local mean sea level

4.2 Stream

There are three USGS stream gages within the study area: 16630200 in Honokowai, 16623500 in Kaopala, and 16623400 in Honokahua. These crest-stage gages provide peak flow data at each site. However, the stream gage in Kaopala has only a single peak flow that is usable in its very short period of record (four years). There is, however, an instantaneous streamflow gage in one of the watersheds adjacent to the study area: 16620000 in Honokohau. This gage provides continuous streamflow data in 5-minute intervals, with a period of record of 30 years (1990 to 2020). It also provides peak flow data for a period of record of 101 years (1914 – 2019, intermittently). All stream monitoring stations referenced in this study are identified in Table 4-2.

Due to the limited availability of streamflow records within the study area, new stream monitoring stations (Photo 4-1) were installed at three sites in 2017, in partnership with West Maui R2R and the State of Hawaii, Department of Land and Natural Resources (DLNR), Commission on Water Resource Management (CWRM). These stations are still operated and maintained by CWRM today (as of March 2020). Cross sections of the three sites were surveyed when the new monitoring stations were installed in September 2017 and again in November 2018.

Photo 4-1: Stream monitoring station, Papua Gulch, Honolua Watershed (2017)

Table 4-2: Stream Station Inventory

Agency	Site Number	Site Name	Period of Record	Drainage Area (mi^2)	Latitude	Longitude
USGS	16630200	Honokowai Stream at Honokowai, Maui, HI	Peak Flow: 1961 – 2009	5.74	20°56'48"	-156°40'47"
USGS	16623500	Kaopala Gulch near Napili, Maui, HI	Peak Flow: 2016 – 2019[1]	0.86	20°58'55"	-156°40'11"
USGS	16623400	Honokeana Gulch near Honokahua, Maui, HI	Peak Flow: 1965 – 1985	0.75	20°59'27"	-156°40'03"
USGS	16620000	Honokohau Stream near Honokohau, Maui, HI	Peak Flow: 1914 – 2019 Instantaneous: 1990 – 2020	4.18	20°57'44"	-156°35'19"
CWRM	6-124	Honokowai Below Confluence	Instantaneous: 2017 – 2020		20.932457	-156.624945
CWRM	6-156	Honokowai Below Dam	Instantaneous: 2017 – 2020[1]	unknown	unknown	unknown
CWRM	6-158	Honolua Above Highway	Instantaneous: 2017 – 2020		21.013493	-156.632455

[1]: usable data is very limited

4.2.1 **Significant Past Flow Events**

Figure 4-1 shows the annual peak flow record at the stream flow gaging station with the longest period of record: USGS 16620000, Honokohau Stream. The historic maximum flow recorded at this gage was 12,200 ft^3/s on September 12, 2018 during Tropical Storm Olivia. This storm was the first tropical cyclone to make landfall on Maui in recorded history. There were no other events of significance in the recent past (within the last 30 years), with the second greatest peak flow occurring on January 28, 1988.

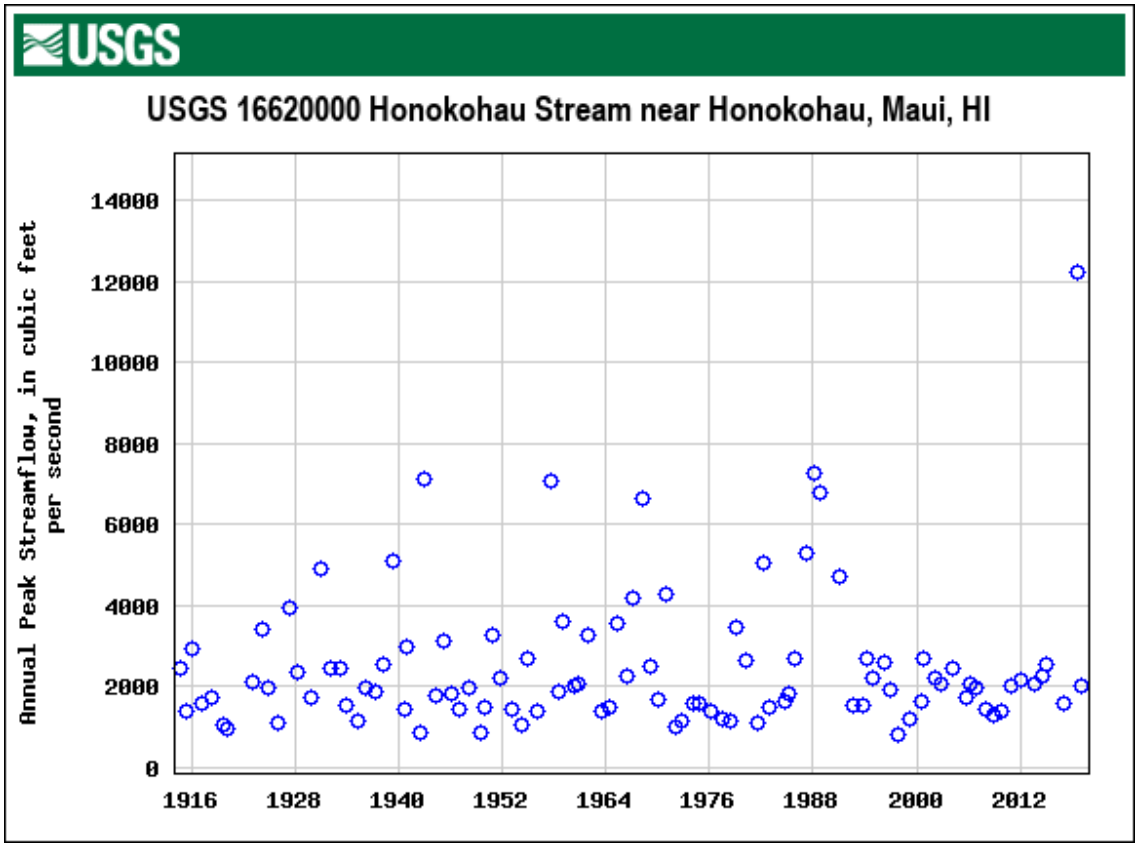

Figure 4-1: Peak stream flow at USGS 16620000

4.3 Sediment

4.3.1 Rainfall Analysis

A rainfall analysis was performed by the USGS to evaluate the frequency of rainfall events that resulted in coastal sediment plumes. Such events were predicted to occur when two or more hours of rain falls at rates greater than 10-20 mm/hr (0.4-0.8 in/hr) in source watersheds. Based on the average rainfall record at the Field 46 and Lahaina climate stations (Table 4-1), two-hour intensities above 10 mm/hr (0.4 in/hr) happened about three times a year in the northern wet side (at Field 46) and about once a year to the south (at Lahaina). These values are slightly lower than the 4-5 times/year recurrence interval suggested by the recent record (2014 – 2016) of the various West Maui R2R climate stations (Table 4-1), located in the southern watersheds. This suggests that West Maui can expect rainfalls that generate plumes to occur between 3 and 5 times a year.

A small number of these storms also have higher rainfall intensities capable of eroding agricultural fields for an hour or longer. These occurred four to five times per decade during the 1980s and 2000s, but only twice during the 1990s. Although past large storms have contributed to sediment loading, annual plume generation is now caused by smaller rainfalls eroding near-stream terrace deposits, a legacy of historic agriculture (Stock & Cerovski-Darriau, 2019).

4.3.2 Field Survey of Historic Fill Terraces

As documented in the 2019 Scientific Investigation Report (SIR) by USGS, *Sediment Budget for Watersheds of West Maui, Hawaii*, the extent of bank erosion was estimated by surveying the extent of historic fill terraces in four valleys: Honokowai Stream, Ka Opala Gulch, lower Honolua Stream, and Papua Gulch (a tributary of Honolua Stream). Surveys showed that fill terraces occupy approximately forty percent (40%) of streambank length (Stock & Cerovski-Darriau, 2019).

4.3.3 **Erosion Pin Test**

As documented in the 2019 Scientific Investigation Report (SIR) by USGS, *Sediment Budget for Watersheds of West Maui, Hawaii*, annual bank erosion rates at four representative sites in the study area were estimated by periodic cross section surveys and erosion pins. At each site, twenty or more long nails were installed at even increments across the channel and pushed or lightly hammered until the rim of the pin was just below the surface. Periodic surveys of each cross section over one year of observation provided approximate lowering rates in the channels at each site. Lowering rates in the higher annual rainfall channels of Honolua and its tributary Papua are much higher than those found at Mahinahina, an ephemeral channel on the "dry side" (Table 4-3). The median lowering rate for all three sites on the "wet side" was estimated to be 14 mm/yr (Stock & Cerovski-Darriau, 2019).

Table 4-3: Annual lowering rates at erosion pin sites

Site	No. observations	Mean (mm/yr)	Standard deviation (mm/yr)
Honolua	40	9.3	8.0
Papua 1	45	15.1	8.7
Papua 2	21	29.0	17.2
Mahinahina	19	4.7	2.2

4.3.4 **Cohesive Strength Meter "Jet" Test**

In 2017, USACE requested assistance from USGS in performing a cohesive strength meter (CSM) test to estimate the cohesive strength of fill terrace sediment (the ability for the sediment to resist shear stress). This test was performed at six locations: the four erosion pin sites, and two additional sites at Honokowai and Mahinahina (Table 4-4). Cohesion values for initiation of bank erosion (90% transmission) at all West Maui fine-grained fill terraces range from 0.2 – 1.2 kPa, with no obvious geographic distribution (

Source: USGS, SIR 2019

Photo 4-2: The Cohesive Strength Meter test deployed at a fill terrace in Wahikuli

Table 4-5). The average value of 0.61 kPa is an estimate for the regional value of bank cohesion at which erosion begins. The average value of 2.68 kPa is an estimate for the regional value of bank cohesion at which substantial erosion occurs (25% transmission).

Table 4-4: CSM test site locations

Location	Latitude	Longitude
Wahikuli Stream	20.913024	-156.688887
Honokowai Stream	20.946716	-156.681593
Mahinahina Gulch	20.958245	-156.679406
Honolua Stream	21.014066	-156.634614
Lower Papua	21.012899	-156.630574
Upper Papua	21.012746	-156.62797

Source: USGS, SIR 2019

Photo 4-2: The Cohesive Strength Meter test deployed at a fill terrace in Wahikuli

Table 4-5: Bank material cohesion

Location	Cohesion							
	90%		75%		50%		25%	
	PSI	kPA	PSI	kPA	PSI	kPA	PSI	kPA
Wahikuli Stream	0.04	0.3	0.09	0.6	0.11	0.8	0.16	1.1
Honokowai Stream	0.06	0.4	0.10	0.7	0.17	1.2	0.36	2.5
Mahinahina Gulch	0.17	1.2	0.29	2.0	0.38	2.6	0.38	2.6
Honolua Stream	0.02	0.2	0.05	0.3	0.22	1.5	0.54	3.7
Lower Papua	0.10	0.7	0.21	1.4	0.22	1.5	0.40	2.7
Upper Papua	0.14	1.0	0.30	2.1	0.30	2.1	0.49	3.4
Average	0.09	0.61	0.17	1.18	0.24	1.62	0.39	2.68

After testing, sediment at each site were analyzed for particle size distribution (Table 4-6; Table 4-7). At some sites, two samples were analyzed.

Table 4-6: Mean and median (D_{50}) particle sizes of fill terrace sediments

Site	Classification	Mean (mm)	Median (mm)	Standard deviation (mm)
Wahikuli	Loam	0.73	0.42	1.09
Honokowai	Silt loam	0.73	0.32	1.22
		0.75	0.31	1.36
Mahinahina	Sandy loam	1.14	0.57	1.63
		0.92	0.48	1.29
Honolua	Silt loam	0.74	0.33	1.29
		0.66	0.34	1.01
Lower Papua	Gravelly sandy loam	0.96	0.48	1.50
Upper Papua	Sandy loam	1.43	0.68	2.30

Table 4-7: Particle size distribution of fill terrace sediment samples by soil classification

Site	Soil texture	Clay	Silt	Very fine sand	Fine sand	Medium sand	Coarse sand	Very coarse sand	Gravel
		< 0.002 mm	0.002-0.05 mm	0.05-0.1 mm	0.1-0.25 mm	0.25-0.5 mm	0.5-1 mm	1-2 mm	> 2 mm
Wahikuli	Loam	7.37	46.00	23.46	14.66	3.49	1.38	0.06	3.58
Honokowai	Silt loam	9.16	52.18	17.25	11.69	4.25	2.15	0.25	3.07
		8.85	51.84	17.81	11.88	4.47	2.05	0.02	3.07
Mahinahina	Sandy loam	6.38	39.77	20.67	20.81	7.64	4.08	0.32	0.33
		6.88	44.19	20.74	19.07	6.45	2.20	0.14	0.33
Honolua	Silt loam	8.93	50.26	19.16	13.34	3.65	2.08	0.21	2.37
		9.06	50.34	20.60	12.65	3.84	1.13	0.02	2.37
Lower Papua	Gravelly sandy loam	5.67	36.91	18.57	14.42	5.15	2.19	0.34	16.75
Upper Papua	Sandy loam	4.85	33.49	21.76	20.94	5.96	4.69	2.11	6.21
	Mean	7.46	45.0	20.0	15.5	4.99	2.43	0.386	4.23

4.3.5 **Sediment Budget**

The final sediment budget estimated by USGS (Table 4-8) indicates that bank erosion of fill terraces from a few watersheds likely dominates the current annual fine sediment load to the nearshore, with Kahana Stream producing the largest annual input of 285 metric tons (Stock & Cerovski-Darriau, 2019).

Table 4-8: USGS sediment budgets for West Maui watersheds

USACE Basin / Subbasin ID	USGS Basin ID	Watershed name	Total area (km^2)	Estimate of annual storm mass load from bank erosion[1] (metric tons/yr)	Hypothetical decadal storm mass load annualized[1] (metric tons/yr)
10	2	Honolua	11.00	91	180
8A	9	Honokahua	6.65	45	37
8B	8	Honokahua	4.03	46	33
7	16	Napili	1.94	43	25
6	20	Ka‘opala	2.36	62	27
5	22	Kahana	11.68	285	125
4	26	Mahinahina	5.00	45	60
3	28	Honokowai	15.20	62	106
2A	30	Hanakaoo	5.94	26	63
2B	31	Hanakaoo	1.65	25	22
1	35	Wahikuli	10.42	42	70
1: assumes 1300 kg/m^3 bulk density					

4.3.6 **Sediment Deposit Samples**

Three surface (0 – 5 cm) soil samples were collected in July 2014 and analyzed for particle size distribution for the *Engineering Analysis and Development of Retrofit Designs of Honokowai Structure #8* (Babcock, et al.). The first sample was collected from within the Mahinahina Basin; the second from a kickout area of an agricultural road above on the Lahaina side of Honokowai Stream; and the third sample was collected from the Ka‘opala Basin. The particle size distribution of the collected samples are provided in Table 4-9.

Table 4-9: Particle Size Distribution of Collected Samples

Sample #	Location	Gravel	Sand	Medium Silt	Small Silt	Clay
1	Mahinahina Basin	5.0	17.2	14.0	15.5	48.3
2	Honokowai Agricultural Road	3.4	23.6	24.7	21.7	26.6
3	Ka‘opala Basin	23.0	57.4	6.2	1.4	12.0

4.3.7 **Sediment Impacts to Coral Reefs**

From a 2011 publication, *Impacts on Sediment on Coral Reefs*, there are essentially three ways in which sediments stress corals: 1) decreasing the available light and thereby also reducing the amount of energy supplied by the zooxanthellae to the coral host; 2) draining their metabolic system as the corals try to rid themselves of the sediment by ciliary action, tentacle waving, or mucus sheet secretion; and 3) increasing bacterial activity and the virulence of disease (Risk & Edinger, pp. 578 - 579). Different sediments exert greatly contrasting levels of stress on the corals, depending on the grain size, organic content, and geochemistry. Clay- and silt-sized sediments have a greater negative impact to corals as they settle more slowly and are more susceptible to resuspension thereby reducing light transmission for a longer period of time (Storlazzi, Norris, & Rosenberger, 2015). Tissue damage under a layer of sediment increases with decreasing grain size (Risk & Edinger, 2011, p. 579). Additionally, finer-grained sediments can be more difficult for coral to remove. A study by Weber et al. (2006) found that photophysiological stress was measureable after 36 hours of exposure to most of the silt-sized sediments, and coral recovery was incomplete after 48 to 96 hours recovery time. In contrast, sandy sediment types caused no measureable stress at the same concentration for the same exposure time. Fine-grained sediments, such as clays and silts, should be targeted for removal for the greatest impact to improving coral health.

5 Flood Frequency Analysis

Methods for estimating the peak flow for the 99%, 50%, 20%, 10%, 4%, 2%, 1%, 0.4%, and 0.2% AEP (1- 2-, 5-, 10-, 25-, 50-, 100-, 200-, and 500-year) flood events (9 profiles) include the following:

1. Stream gage analysis
2. Regional regression equations
3. Rainfall-runoff model

Other peak flow estimates previously published (for reference):

1. 2015 Flood Insurance Study (FIS)

5.1 Stream Gage Analysis

5.1.1 Bulletin 17B

Annual peak flow data from the two stream gages within the watershed were analyzed individually using methodology from Bulletin 17B (Interagency Advisory Committe on Water Data, 1982) as applied by the Hydrologic Engineering Center's Statistical Software Package (HEC-SSP) program (version 2.2, HEC, 2019) which follows the Bulletin 17B guidance. The weighted skew option was used, which weights the computed station skew with the generalized regional skew. A generalized skew value of -0.05 and mean-square error of 0.302 was used per the national map in Bulletin 17B and verified by USGS in 2010 (Oki, Rosa, & Yeung). Table 5-1 contains the number and names of the stream-gaging stations upon which a Bulletin 17B analysis was performed.

Table 5-1: Relevant stream gages

Site Number	Site Name	Period of record	No. years of usable record	Drainage area (mi^2)
16630200	Honokowai Stream at Honokowai, Maui, HI	1961 – 2009	47	5.74
16623400	Honokeana Gulch near Honokahua, Maui, HI	1965 – 1985	22	0.75
16620000	Honokohau Stream near Honokohau, Maui, HI	1914 – 2019	101	4.18

Table 5-2, Table 5-3, and Table 5-4 present the resulting peak flow estimates for USGS 16630200, 16623400, and 16620000, respectively.

Table 5-2: Peak flow estimates computed using Bulletin 17B methodology at USGS 16630200, Honokowai Watershed

Annual Exceedance Probability (AEP)	Computed Curve Flow in ft^3/s	Confidence Limits	
		0.05	0.95
1/500	6,469	11,171	4,348
1/200	4,805	7,839	3,358
1/100	3,783	5,901	2,726
1/50	2,932	4,364	2,180
1/25	2,226	3,156	1,709
1/10	1,476	1,957	1,182
1/5	1,022	1,288	842
1/2	530	635	440
1/1	116	154	79.3

Table 5-3: Peak flow estimates computed using Bulletin 17B methodology on USGS 16623400, Honokahua Watershed

Annual Exceedance Probability (AEP)	Computed Curve Flow in ft^3/s	Confidence Limits	
		0.05	0.95
1/500	7,521	60,262	1,971
1/200	5,098	36,375	1,422
1/100	3,609	23,267	1,063
1/50	2,410	13,833	754
1/25	1,487	7,463	498
1/10	656	2,653	243
1/5	280	928	113
1/2	43.3	107	18.1
1/1	0	0.2	0

Table 5-4: Peak flow estimates computed using Bulletin 17B methodology on USGS 16620000, Honokohau Watershed

Annual Exceedance Probability (AEP)	Computed Curve Flow in ft^3/s	Confidence Limits	
		0.05	0.95
1/500	14,305	18,690	11,537
1/200	11,133	14,105	9,195
1/100	9,127	11,291	7,678
1/50	7,408	8,944	6,350
1/25	5,935	6,989	5,184
1/10	4,300	4,898	3,848
1/5	3,250	3,616	2,956
1/2	2,018	2,201	1,847
1/1	779	890	663

5.1.2 **Bulletin 17C**

The Bulletin 17B analysis discussed in the previous section relies primarily on systematic records represented as point observations, i.e. peak discharge values recorded by one of two gaging stations. A Bulletin 17C analysis offers the opportunity to also use intervals or thresholds to represent the magnitudes of flood peaks that might be known with less precision, such as historical flood data. There is no known additional historical flood data to add to the record. Thresholds were added to indicate all other floods that may have occurred during data gaps in the record.

Table 5-5, Table 5-6, and Table 5-7 contain the results from completing a Bulletin 17C analysis at the three gage locations. The same generalized skew value of -0.05 and mean-square error of 0.302 were used.

Table 5-5: Peak flow estimates computed using Bulletin 17C methodology for USGS 16630200, Honokowai Watershed

Annual Exceedance Probability (AEP)	Computed Curve Flow in ft^3/s	Variance Log	Confidence Limits	
			0.05	0.95
1/500	6,469	0.03554	20,009	3,796
1/200	4,805	0.02506	12,084	3,044
1/100	3,784	0.01857	8,185	2,533
1/50	2,932	0.01329	5,498	2,069
1/25	2,226	0.00917	3,655	1,648
1/10	1,476	0.00538	2,087	1,155
1/5	1,022	0.00364	1,328	826
1/2	530	0.00251	645	438
Station Skew: 0.516 | Regional Skew: -0.050 | Weighted Skew: 0.330				

Table 5-6: Peak flow estimates computed using Bulletin 17C methodology for USGS 16623400, Honokahua Watershed

Annual Exceedance Probability (AEP)	Computed Curve Flow in ft^3/s	Variance Log	Confidence Limits	
			0.05	0.95
1/500	2,764	0.13327	37,422	1,000
1/200	1,918	0.10166	17,437	781
1/100	1,412	0.08062	9,527	625
1/50	1,004	0.06207	4,941	484
1/25	683	0.04607	2,460	357
1/10	371	0.02917	914	214
1/5	206	0.02054	408	124
1/2	64.2	0.02226	103	16.9
Station Skew: -0.564 | Regional Skew: -0.050 | Weighted Skew: -0.169				

Table 5-7: Peak flow estimates computed using Bulletin 17C methodology for USGS 16620000, Honokohau Watershed

Annual Exceedance Probability (AEP)	Computed Curve Flow in ft^3/s	Variance Log	Confidence Limits	
			0.05	0.95
1/500	14,305	0.01374	27,722	10,198
1/200	11,133	0.00934	18,943	8,380
1/100	9,127	0.00668	14,137	7,148
1/50	7,409	0.00456	10,502	6,024
1/25	5,935	0.00295	7,758	4,998
1/10	4,300	0.00155	5,140	3,767
1/5	3,250	0.00096	3,704	2,912
1/2	2,018	0.00061	2,221	1,838
Station Skew: 0.796 | Regional Skew: -0.050 | Weighted Skew: -0.422				

5.2 Regional Regression Equations

In 2010, the U.S. Geological Survey published *Flood Frequency Estimates for Streams on Kaua'i, O'ahu, Moloka'i, Maui, and Hawaii, State of Hawaii*, which includes regional regression equations for estimating peak flow for the 50%, 20%, 10%, 4%, 2%, 1%, and 0.2% AEP (2-, 5-, 10-, 25-, 50-, 100-, and 500-year) flood events (7 profiles). The Wahikuli, Hanakaoo, and Honokowai watersheds are located in the central-southwestern region of Maui, *Region 7*, and the other watersheds in the study area are located in the eastern-northwestern region of Maui, *Region 8*. The equations for each region are presented in Table 5-8 and Table 5-9, respectively. Results of using these equations to estimate peak flow at each subbasin are presented in Table 5-10 through Table 5-11.

Table 5-8: Regional regression equations for peak flow estimates in Region 7

Regression equation	Range of explanatory variables	Standard error of prediction, in percent	R^2	Standard model error, in percent
$Q_2=55.46\ (DA^{0.506})$	$0.45 \leq DA \leq 18.6$	320	0.07	270
$Q_5=162.9(DA^{0.638})$	$0.45 \leq DA \leq 18.6$	99	0.50	87
$Q_{10}=276.7(DA^{0.691})$	$0.45 \leq DA \leq 18.6$	62	0.73	52
$Q_{25}=463.4(DA^{0.731})$	$0.45 \leq DA \leq 18.6$	55	0.80	44
$Q_{50}=638.3(DA^{0.750})$	$0.45 \leq DA \leq 18.6$	59	0.79	48
$Q_{100}=843.3(DA^{0.764})$	$0.45 \leq DA \leq 18.6$	67	0.76	54
$Q_{500}=1{,}459(DA^{0.787})$	$0.45 \leq DA \leq 18.6$	89	0.71	73

Q_T = peak discharge for T-year recurrence interval

DA = drainage area, in square miles

$a < DA < b$ = the drainage area may be greater than or equal to a and less than or equal to b

Table 5-9: Regional regression equations for peak flow estimates in Region 8

Regression equation	Range of explanatory variables	Standard error of prediction, in percent	R^2	Standard model error, in percent
$Q_2=602.6(DA^{0.885})$	$0.09 \leq DA \leq 17.2$	93	0.64	90
$Q_5=1038(DA^{0.831})$	$0.09 \leq DA \leq 17.2$	70	0.71	68
$Q_{10}=1380(DA^{0.804})$	$0.09 \leq DA \leq 17.2$	66	0.72	64
$Q_{25}=1875(DA^{0.776})$	$0.09 \leq DA \leq 17.2$	65	0.72	63
$Q_{50}=2280(DA^{0.759})$	$0.09 \leq DA \leq 17.2$	67	0.71	65
$Q_{100}=2716(DA^{0.744})$	$0.09 \leq DA \leq 17.2$	70	0.69	67
$Q_{500}=3,828(DA^{0.717})$	$0.09 \leq DA \leq 17.2$	79	0.64	76

Q_T = peak discharge for T-year recurrence interval

DA = drainage area, in square miles

$a < DA < b$ = the drainage area may be greater than or equal to a and less than or equal to b

Table 5-10: Peak flow estimates at various basin outlets, computed using regional equations

Basin ID	Drainage area (mi^2)	Region	Peak flow (ft^3/s)[1]						
			1/2	1/5	1/10	1/25	1/50	1/100	1/500
1	3.89	7	110	388	707	1,250	1,770	1,800	4,250
2	3.37	7	103	354	641	1,130	1,590	1,610	3,800
3	5.80	7	135	500	932	1,680	2,390	2,450	5,820
4	1.80	8	74.7	237	415	712	992	1,000	2,320
5	4.35	8	117	416	764	1,360	1,920	1,960	4,640
6	0.812	8	49.9	143	240	398	546	544	1,240
7	1.80	8	74.7	237	415	712	992	1,000	2,320
8	4.13	8	114	403	737	1,310	1,850	1,890	4,450
10	4.28	8	116	412	756	1,340	1,900	1,940	4,580
12	4.32	8	2,200	3,500	4,480	5,840	6,920	8,070	10,900

[1]: rounded to three significant figures

Table 5-11: Subbasin peak flow estimates, computed using regional equations

Subbasin ID	Drainage area (mi^2)	Peak flow (ft^3/s)[1]						
		1/2	1/5	1/10	1/25	1/50	1/100	1/500
1A	0.237	26.8	65.0	102	162	217	212	470
1B	2.28	84.2	276	489	846	1,180	1,200	2,790
1C	1.37	65.0	199	344	583	808	812	1,870
2A	0.679	45.6	127	212	349	477	475	1,080
2B	2.69	91.5	306	548	955	1,340	1,360	3,180
3A	0.243	27.1	66.1	104	165	221	217	479
3B	1.56	69.5	216	376	641	891	897	2,070
3C	1.77	74.0	234	411	703	980	987	2,290
3D	2.23	83.2	272	482	833	1,160	1,180	2,740
4A	1.80	1,010	1,690	2,210	2,960	3,560	4,210	5,830
5A	0.060	50.0	100	144	211	269	335	509
5B	1.36	791	1,340	1,770	2,380	2,880	3,410	4,770
5C	2.92	1,560	2,530	3,270	4,310	5,140	6,030	8,250
6A	0.812	501	873	1,170	1,600	1,950	2,330	3,300
7A	0.554	357	635	858	1,190	1,460	1,750	2,510
8A	2.60	1,400	2,300	2,980	3,940	4,710	5,530	7,590
8B	1.53	878	1,480	1,940	2,610	3,150	3,730	5,190
10A	0.386	260	471	642	896	1,110	1,340	1,930
10B	2.78	1,490	2,430	3,140	4,150	4,950	5,810	7,970
10C	1.11	661	1,130	1,500	2,030	2,470	2,940	4,130
12A	4.32	2,200	3,500	4,480	5,840	6,920	8,070	10,900

[1]: rounded to three significant figures

Table 5-12: Peak flow estimates for key locations in the study area, computed using regional equations

Location	Drainage area (mi^2)	Region	Peak flow (ft^3/s)[1]						
			1/2	1/5	1/10	1/25	1/50	1/100	1/500
CWRM 6-124	2.23	7	83.2	272	482	833	1,160	1,180	2,740
CWRM 6-158	3.89	8	110	388	707	1,250	1,770	1,800	4,250
Wahikuli Junction	3.65	7	107	372	677	1,190	1,690	1,720	4,040
Honokowai Dam	5.56	7	132	487	905	1,620	2,310	2,370	5,630
Kahana Dam	4.28	8	116	412	756	1,340	1,900	1,940	4,580
USGS -0000	4.18	8	114	406	743	1,320	1,870	1,900	4,500
USGS -0200	5.74	7	134	497	926	1,660	2,370	2,430	5,770
USGS -3400	0.75	8	47.9	136	227	376	514	512	1,160
[1]: rounded to three significant figures									

5.3 Rainfall-Runoff Model

The discharge-frequency relationships at key points in the study area were determined by developing rainfall-runoff models for ten watersheds using the Hydrologic Engineering Center's Hydrologic Modeling System (HEC-HMS, version 4.3, 2019) software. The ten watersheds selected are: Wahikuli, Hanakaoo, Honokowai, Mahinahina, Kahana, Kaopala, Napili, Honokohua, Honolua, and Honokohau (adjacent to the study area). These watersheds were selected primarily due to their size (drainage area), availability of historical streamflow data (Section 4.2), likelihood for mitigation measures to be implemented (e.g. grant opportunities, existing land owner partnerships), and for their collective ability to represent the entire study area well. It was not possible to calibrate this model effectively to specific historical storm events due to the limited number of sites and storm events in the available record. However, a Bulletin 17B stream gage analysis on two sites in the Honokohau and Honokowai watershed (Section 5.1.1) provided a strong level of confidence based on long periods of record and the rainfall-runoff model was calibrated to match these results. The calibrated peak flow estimates computed by the rainfall-runoff model were "adopted" as the final peak flow estimates to be carried forward for use in this study and are presented in Section 5.3.

5.3.1 **Basin Characteristics**

GIS data were used to delineate the basins (Table 5-13), subbasins (Table 5-14) and rivers. Each basin was divided into subbasins based on key locations in the watershed (e.g. the location of a streamflow gage, junction, or existing detention basin). The basin model layout created in HEC-HMS is provided in Figure 5-1.

Table 5-13: Basin identification and information

Basin ID	Basin name	Drainage area (mi^2)	Centroid location	
			Latitude	Longitude
1	Wahikuli	3.89	20.911475	-156.639656
2	Hanakaoo	3.37	20.928895	-156.657939
3	Honokowai	5.80	20.929811	-156.632436
4	Mahinahina	1.80	20.948749	-156.650262
5	Kahana	4.35	20.952354	-156.635833
6	Kaopala	0.812	20.967475	-156.642701
7A	Honokeana	0.554	20.978622	-156.652712
7B	Napili 4-5	0.814	20.974488	-156.640926
7C	Napili 2-3	0.433	20.983515	-156.646616
8	Honokohua	4.13	20.975677	-156.629628
10	Honolua	4.28	20.976841	-156.615055
12	Honokohau	4.32	20.927803	-156.585456

Table 5-14: Subbasin identification and information

Subbasin ID	Basin name	Drainage area (mi^2)	Centroid location	
			Latitude	Longitude
1A	Wahikuli	0.237	20.914075	-156.68211
1B	Wahikuli	2.28	20.909011	-156.635398
1C	Wahikuli	1.37	20.915133	-156.639399
2A	Hanakaoo	0.679	20.929989	-156.673387
2B	Hanakaoo	2.69	20.928619	-156.654040
3A	Honokowai	0.243	20.947352	-156.683530
3B	Honokowai	1.56	20.930424	-156.641111
3C	Honokowai	1.77	20.941118	-156.650151
3D	Honokowai	2.23	20.918459	-156.606669
4A	Mahinahina	1.80	20.948749	-156.650262
5A	Kahana	0.060	20.97671	-156.673711
5B	Kahana	1.36	20.956836	-156.648874
5C	Kahana	2.92	20.949757	-156.628927
6A	Kaopala	0.812	20.967475	-156.642701
7A	Honokeana	0.554	20.978622	-156.652712
7B	Napili 4-5	0.814	20.974488	-156.640926
7C	Napili 2-3	0.433	20.983515	-156.646616
8A	Honokohua	2.60	20.971047	-156.629524
8B	Honokohua	1.53	20.983527	-156.629806
10A	Honolua	0.386	21.008828	-156.632857
10B	Honolua	2.78	20.965825	-156.611664
10C	Honolua	1.11	20.993317	-156.617362
12A	Honokohau	4.32	20.927803	-156.585456

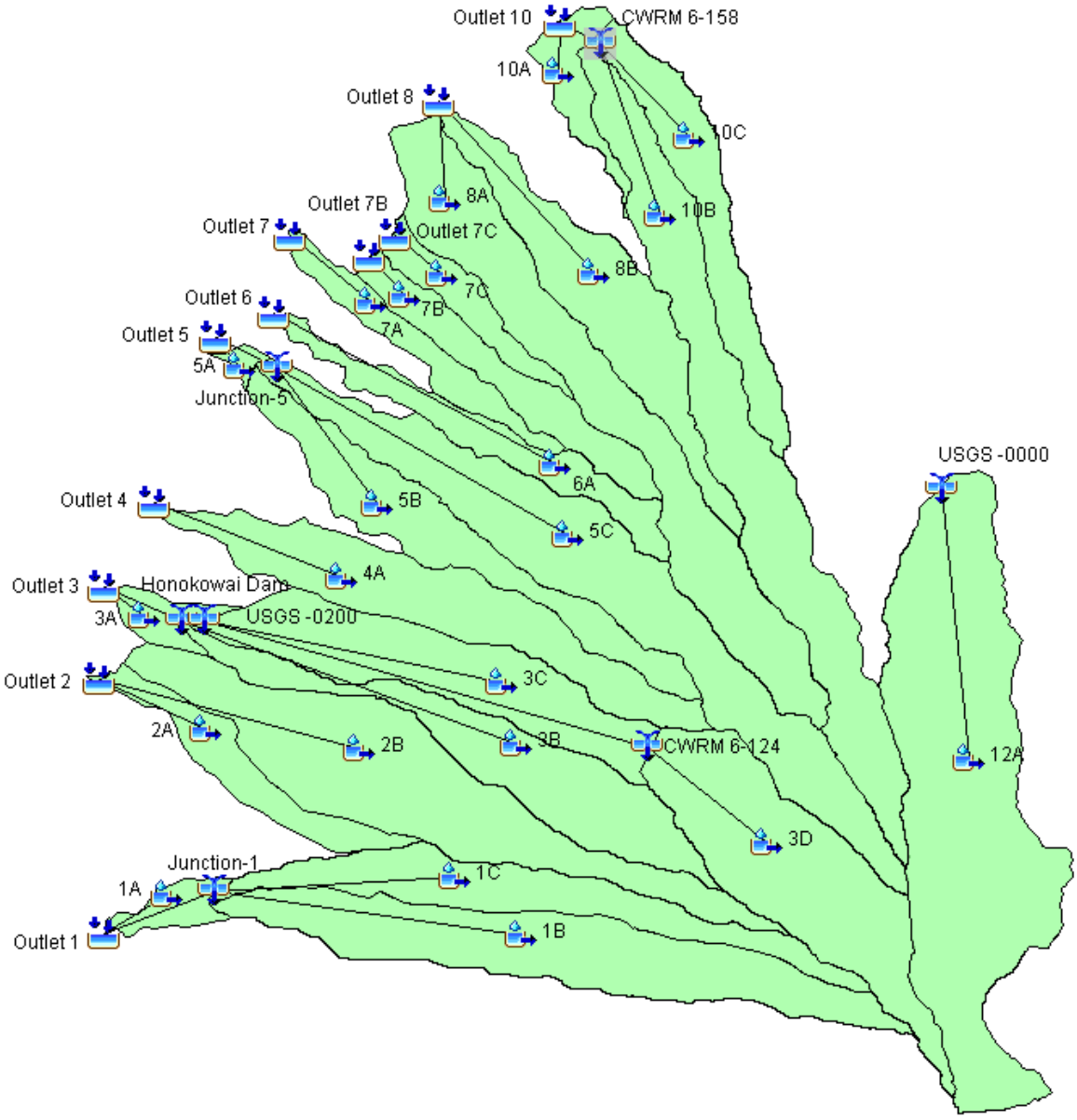

Figure 5-1: HEC-HMS Basin Model Layout

5.3.2 **Initial estimation for loss parameters**

The initial and constant loss methods were applied to the model to account for precipitation loss due to infiltration. This approach uses three parameters: initial loss, constant rate, and percent impervious area. The initial loss, the amount of precipitation lost to the soil at the beginning of the rainfall event, depends on the saturation of the soil and varies for each event. 0.1 inches of precipitation was assumed to be the initial loss due to absorption of the soil.

The constant loss rates were determined using soil data from the Hawai'i Soil Data Atlas, an interactive and online tool for providing basic information about each soil type (University of Hawai'i, 2014). Each soil type had previously been classified by their saturated hydraulic conductivity (Ksat) as either slow (< 3 micrometers per second; µm/s), moderate (3 to 10 µm/s), fast (10 to 100 µm/s), or very fast (> 100 µm/s). Only fast and moderate soil types were found in the study area. A geospatial shapefile provided by the Hawai'i Soil Data Atlas was used to compute a weighted average Ksat for each subbasin, and then converted to the appropriate units – inches per hour (in/hr). Results are provided in Table 5-15.

Table 5-15: Initial constant loss rates

Subbasin ID	Saturated hydraulic conductivity, Ksat (μm/s)	Constant loss rate (in/hr)
1A	9.47	1.34
1B	20.7	2.93
1C	22.1	3.13
2A	13.9	1.96
2B	17.8	2.52
3A	13.0	1.84
3B	15.2	2.15
3C	12.7	1.80
3D	39.9	5.65
4A	14.8	2.10
5A	13.7	1.95
5B	19.0	2.70
5C	29.4	4.17
6A	19.1	2.71
7A	13.0	1.84
7B	17.1	2.43
7C	15.7	2.22
8A	30.4	4.31
8B	25.5	3.61
10A	18.4	2.60
10B	36.0	5.10
10C	25.8	3.65
12A	29.2	4.13

NRCS's Technical Release 55 (TR-55) identifies typical percentages of directly connected impervious areas (DCIA) for various land cover types. A land cover raster (Section 3.5) was used to compute the weighted average DCIA based on the various land cover classifications (Table 5-16) within each subbasin. Results are provided in Table 5-17.

Table 5-16: Directly connected impervious areas by land cover type

Land cover	Directly connected impervious area (%)
Developed, Open Space	< 20
Developed, Low Intensity	20 – 49
Developed, Medium Intensity	50 – 79
Developed, High Intensity	80 – 100

Table 5-17: Directly connected impervious areas for each subbasin

Subbasin ID	Directly connected impervious area (%)
1A	7.87
1B	0.443
1C	0.150
2A	4.55
2B	1.52
3A	18.74
3B	0.827
3C	1.80
3D	0.031
4A	3.02
5A	24.8
5B	2.35
5C	0.809
6A	1.71
7A	10.7
7B	14.6

7C	22.7
8A	3.27
8B	1.69
10A	5.32
10B	0.417
10C	0.583
12A	0.017

5.3.3 **Initial estimation for transform parameters**

The excess precipitation in each subbasin was transformed into surface runoff by applying the SCS Unit Hydrograph method in the hydrologic model. This method was selected because it requires only a single parameter (Lag time, t_L) that could easily be determined based on the GIS data available for the study area. Other transform methods, such as Clark's Unit Hydrograph, would be difficult to apply as it relies upon distinguishing between sheet, shallow, and channel flow using elevation data that does not define channels clearly in the middle and upper watershed. t_L represents the time between the center of the mass of rainfall excess (about in the middle of the rainfall event) to the peak discharge (when there is the greatest amount of flow in the channel) and was estimated using the SCS lag equation, given as:

$$t_L = \frac{L^{0.8}(S+1)^{0.7}}{1900\,(Y)^{0.5}}$$

where: t_L = lag time in hours (hrs)

L = length of the longest drainage path in feet (ft)

S = potential maximum retention in inches, (1000/CN)-10

CN = the average curve number for the subbasin

Y = the average subbasin slope in percent (%)

The average curve number for the subbasin, CN, was determined by using the general land cover and land use raster (Section 3.5) and soil properties shapefile (Section 3.6). Individual curve numbers were assigned to specific areas based on their land cover classification and hydrologic soil group, as presented in Table 5-18 (NRCS, 1986).

The average subbasin slope was determined by creating a slope raster from the USGS NED raster (Section 3.2) and then applying the "Zonal Statistics" tool to calculate the average slope for each subbasin.

Table 5-18: Representative curve numbers for various land cover types

NLCU ID	Land cover description	CN ID	CN description	Hydrologic soil group			
				A	B	C	D
2	Developed, High Intensity	2	Urban: commercial	89	92	94	95
3	Developed, Medium Intensity	3	Residential: 1/8 acre lot	61	75	83	87
4	Developed, Low Intensity	4	Residential: 1/3 acre lot	57	72	81	86
5	Developed, Open Space	5	Open space, fair condition	49	69	79	84
6	Cultivated Crops	6	Fallow: crop residue cover	76	85	90	93
20	Bare Land	20	Fallow: bare soil	77	86	91	94
7	Pasture / Hay	7	Pasture, grassland, or range	49	69	79	84
8	Grassland / Herbaceous						
12	Scrub / Shrub						
10	Evergreen Forest	10	Woods	30	48	65	73
13	Palustrine Forested Wetland	13	Water / wetland	0	0	0	0
14	Palustrine Scrub / Shrub Wetland						
15	Palustrine Emergent Wetland						
21	Open Water						

The computed lag times for each subbasin are presented in Table 5-19, along with selected peak rating factors (PRFs). Steep terrain and urban areas tend to produce higher and earlier peaks than flat, swampy regions. The default PRF of 484 can be adjusted in the hydrologic model to something more representative of the basin. Table 5-20 provides some guidance for the selection of this parameter (NWS, 2005). Generally, the average watershed slope (Y) and general land cover classification influenced the PRF selected for each subbasin.

Table 5-19: Lag time estimates for each subbasin

Subbasin ID	L	CN	S	Y	t_L	PRF
1A	5,640	87.4	1.44	11.7	0.288	400
1B	33,576	64.4	5.53	48	1.18	484
1C	31,178	66	5.15	41.7	1.14	484
2A	16,941	89.3	1.20	7.25	0.82	400
2B	34,408	79.6	2.56	21.5	1.18	484
3A	3,953	91.8	0.89	7.32	0.229	400
3B	27,599	68	4.71	33.7	1.1	484
3C	23,514	79.9	2.52	39.5	1.74	484
3D	21,747	41.1	14.33	82.7	3.13	550
4A	27,940	81.2	2.32	21.6	0.946	484
5A	2,756	85.6	1.68	8.35	0.205	400
5B	27,456	76.6	3.05	22.9	1.04	400
5C	40,729	58.8	7.01	50	1.56	500
6A	17,965	71.5	3.99	28.6	0.768	400
7A	15,869	86.1	1.61	16.9	0.575	400
7B	16,810	74.4	3.44	24.3	1.93	400
7C	10,825	80.3	2.45	19.3	1.22	400
8A	36,527	55.1	8.15	44.5	1.66	484
8B	25,659	60.3	6.58	34.2	1.25	484
10A	6,097	80.8	2.38	17.5	0.315	400
10B	44,438	45.2	12.12	53.4	2.28	500
10C	21,561	57.9	7.27	41.3	1.05	484
12A	32,282	46.8	11.37	87.8	1.33	550

Table 5-20: Hydrograph peaking factors and recession limb ratios:

General description	Peaking factor	Limb ratio (recession to rising)
Urban areas; steep slopes	575	1.25
Typical SCS	484	1.67
Mixed urban/rural	400	2.25
Rural, rolling hills	300	3.33
Rural, slight slopes	200	5.5
Rural, very flat	100	12.0

5.3.4 **Model Calibration**

The model was initially calibrated to replicate specific historical storms; however, the limited number of sites and storm events that could be used for calibration proved this method to be ineffectual. Four events were selected for calibration: October 24, 2017; December 20, 2017; February 18, 2018; and September 18, 2018 (Tropical Storm Olivia). Apart from Tropical Storm Olivia, there were no significant events (events greater than a 10% annual exceedance probability) in the last 30 years. Despite extreme adjustments to the loss and transform parameters, the rainfall-runoff was not able to replicate the peak flows recorded during the February 2018 and September 2018 storm events. This was likely due to an inaccurate representation of rainfall over the study area, which was based on records from the Puu Kukui climate station. For example, Tropical Storm Olivia was centered west of the Puu Kukui climate station and it is likely that more precipitation fell on the study area than was recorded by the station.

However, a Bulletin 17C stream gage analysis on two sites in the Honokohau and Honokowai watershed (Section 5.1.2) provided a strong level of confidence based on long periods of record and the rainfall-runoff model was calibrated to match these results.

5.3.4.1 Precipitation Frequency Data

Point precipitation data was obtained from the National Weather Service's (NWS) NOAA Atlas 14 Precipitation-Frequency Data Server (PFDS). This source presents the estimated total rainfall from recurrence intervals of 1 to 1000 years (100% to 0.1% annual exceedance probabilities) for various durations (5 minutes to 60 days) within or adjacent

to the study area (NOAA, 2017). The location points used to extract PFDS data were the approximate centroid locations for each subbasin (Table 3-3).

5.3.4.2 Calibrated Parameters

The peak flow at the HEC-HMS element representing the USGS stream gage in Honokohau (USGS -0000) is dependent on the parameters of subbasin 12A, and the peak flow at the element representing USGS stream gage in Honokowai (USGS -0200) is dependent on the parameters of subbasins 3C and 3D. The *constant loss* parameters of these subbasins were adjusted until the model was able to closely match the estimated peak flow for each frequency event (e.g. the 1/100 AEP event) as determined by the corresponding Bulletin 17B results. Calibrated values for the constant loss parameter, as presented in Table 5-21 and Table 5-22, varied for each frequency event and were characterized by the percent change from its initial value.

Table 5-21: Calibrated "constant loss" parameter for subbasin 12A

AEP Event	Constant loss (in/hr)		Peak flow (ft^3/s)	
	Value	Percent change	Calibrated	Bulletin 17B
Initial	4.13	0.0	--	--
1/500	1.72	-58.4	14,921	14,305
1/200	2.10	-49.2	11,061	11,133
1/100	2.23	-46.0	9,138	9,127
1/50	2.35	-43.1	7,408	7,408
1/25	2.41	-41.6	5,932	5,935
1/10	2.51	-39.2	4,296	4,300
1/5	2.59	-37.3	3,255	3,250
1/2	2.65	-35.8	2,021	2,018

Table 5-22: Calibrated "constant loss" for subbasins 3C and 3D

AEP Event	Constant loss (in/hr)			Peak flow (ft^3/s)	
	3C Value	3D Value	Percent change	Calibrated	Bulletin 17B
Initial	1.80	5.65	0.0	--	--
1/500	0.347	1.091	-80.7	6,473	6469
1/200	0.540	1.70	-70.0	4,683	4805
1/100	0.652	2.05	-63.8	3,783	3783
1/50	0.743	2.33	-58.7	2,934	2932
1/25	0.833	2.62	-53.7	2,228	2226
1/10	0.943	2.96	-47.6	1,476	1476
1/5	1.035	3.25	-42.5	1,022	1022
1/2	1.242	3.90	-31.0	530	530

The percent change of each calibrated "constant loss" value from its initial estimate in Honokohau and Honokowai were used to adjust the initial estimates of other subbasins in the study area. With "0" representing the percent change value at the dry, western subbasins of Honokowai, and "1" representing the percent change value at the wet, northern subbasin of Honokohau, a scale factor was assigned to each subbasin based on the azimuths from a central point (the highest peak in the Honokohau watershed) to the centroid of each subbasin (Table 5-23). For the Wahikuli and Hanakaoo watersheds, which are beyond this range (Honokowai to Honokohau), the same scale factor and percent change that were used for Honokowai were also applied to these watersheds. Final adjusted constant loss values for each subbasin are presented in Table 5-24.

Table 5-23: Assigned scale factors and percent changes for each subbasin

Subbasin ID	Azimuth (º)	Scale factor	Percent change from initial value (%)							
			1/500	1/200	1/100	1/50	1/25	1/10	1/5	1/2
1A	165.3279	0.00	-80.7	-70.0	-63.8	-58.7	-53.7	-47.6	-42.5	-31
1B	158.1414	0.00	-80.7	-70.0	-63.8	-58.7	-53.7	-47.6	-42.5	-31
1C	153.7315	0.00	-80.7	-70.0	-63.8	-58.7	-53.7	-47.6	-42.5	-31
2A	154.2448	0.00	-80.7	-70.0	-63.8	-58.7	-53.7	-47.6	-42.5	-31
2B	149.092	0.00	-80.7	-70.0	-63.8	-58.7	-53.7	-47.6	-42.5	-31
3A	148.1117	0.00	-80.7	-70.0	-63.8	-58.7	-53.7	-47.6	-42.5	-31
3B	142.2301	0.00	-80.7	-70.0	-63.8	-58.7	-53.7	-47.6	-42.5	-31
3C	139.8578	0.00	-80.7	-70.0	-63.8	-58.7	-53.7	-47.6	-42.5	-31
3D	124.422	0.00	-80.7	-70.0	-63.8	-58.7	-53.7	-47.6	-42.5	-31
4A	135.909	1.53	-87.9	-76.7	-69.5	-63.7	-57.6	-50.3	-44.2	-29.5
5A	133.6208	1.50	-86.5	-75.4	-68.4	-62.7	-56.8	-49.8	-43.8	-29.8
5B	131.5655	1.48	-85.2	-74.2	-67.4	-61.8	-56.1	-49.3	-43.5	-30.0
5C	124.0752	1.40	-80.5	-69.8	-63.6	-58.5	-53.6	-47.5	-42.4	-31.0
6A	124.5628	1.40	-80.8	-70.1	-63.9	-58.8	-53.7	-47.6	-42.5	-31.0
7A	125.3171	1.41	-81.3	-70.5	-64.2	-59.1	-54.0	-47.8	-42.6	-30.9
7B	121.4476	1.37	-78.8	-68.3	-62.3	-57.4	-52.7	-46.9	-42.1	-31.4
7C	121.3696	1.37	-78.8	-68.2	-62.3	-57.4	-52.7	-46.9	-42.1	-31.4
8A	116.7817	1.31	-75.9	-65.5	-60.0	-55.4	-51.1	-45.8	-41.4	-32.0
8B	113.7432	1.28	-74.0	-63.8	-58.5	-54.0	-50.1	-45.1	-40.9	-32.4
10A	110.309	1.24	-71.9	-61.8	-56.7	-52.5	-48.9	-44.3	-40.4	-32.9
10B	107.585	1.21	-70.1	-60.2	-55.4	-51.3	-48.0	-43.6	-40.0	-33.3
10C	105.8733	1.19	-69.1	-59.2	-54.5	-50.6	-47.4	-43.2	-39.8	-33.5
12A	88.8366	1.00	-58.4	-49.2	-46.0	-43.1	-41.6	-39.2	-37.3	-35.8

Table 5-24: Adjusted constant loss values for each subbasin

Subbasin ID	Initial	Constant loss (in/hr)							
		1/500	1/200	1/100	1/50	1/25	1/10	1/5	1/2
1A	1.34	0.259	0.402	0.485	0.553	0.620	0.702	0.771	0.925
1B	2.93	0.565	0.879	1.061	1.210	1.357	1.535	1.685	2.022
1C	3.13	0.604	0.939	1.133	1.293	1.449	1.640	1.800	2.160
2A	1.96	0.378	0.588	0.710	0.809	0.907	1.027	1.127	1.352
2B	2.52	0.486	0.756	0.912	1.041	1.167	1.320	1.449	1.739
3A	1.84	0.355	0.552	0.666	0.760	0.852	0.964	1.058	1.270
3B	2.15	0.415	0.645	0.778	0.888	0.995	1.127	1.236	1.484
3C	1.8	0.347	0.540	0.652	0.743	0.833	0.943	1.035	1.242
3D	5.65	1.090	1.695	2.045	2.333	2.616	2.961	3.249	3.899
4A	2.1	0.254	0.489	0.640	0.762	0.890	1.043	1.172	1.482
5A	1.95	0.264	0.480	0.616	0.727	0.842	0.979	1.095	1.370
5B	2.7	0.400	0.697	0.881	1.031	1.185	1.369	1.524	1.889
5C	4.17	0.814	1.259	1.517	1.729	1.936	2.188	2.400	2.875
6A	2.71	0.521	0.811	0.979	1.118	1.253	1.419	1.558	1.870
7A	1.84	0.345	0.542	0.658	0.753	0.846	0.960	1.056	1.272
7B	2.43	0.514	0.771	0.916	1.035	1.150	1.290	1.408	1.667
7C	2.22	0.471	0.706	0.838	0.947	1.051	1.179	1.286	1.523
8A	4.31	1.038	1.485	1.725	1.924	2.107	2.336	2.526	2.929
8B	3.61	0.938	1.308	1.500	1.660	1.803	1.983	2.132	2.439
10A	2.6	0.732	0.994	1.125	1.235	1.329	1.449	1.549	1.745
10B	5.1	1.522	2.032	2.276	2.483	2.653	2.875	3.058	3.403
10C	3.65	1.129	1.491	1.660	1.804	1.920	2.072	2.198	2.427
12A	4.13	1.718	2.098	2.230	2.350	2.412	2.511	2.590	2.651

5.4 Final Peak Flow Estimates

The calibrated peak flow estimates computed by the rainfall-runoff model were "adopted" as the final peak flow estimates to be carried forward for use in this study. These estimates are provided in Table 5-25 through Table 5-27.

Table 5-25: Peak flow estimates at each basin outlet

Basin ID	Peak flow (ft^3/s)[1]							
	1/2	1/5	1/10	1/25	1/50	1/100	1/200	1/500
1	1,270	2,330	3,220	4,740	6,080	7,460	9,010	11,400
2	667	1,370	1,980	3,030	4,020	5,080	6,290	8,170
3	646	1,190	1,710	2,580	3,340	4,220	5,320	7,230
4	453	933	1,360	2,070	2,690	3,340	4,090	5,180
5	496	1,100	1,690	2,670	3,650	4,840	6,290	8,630
6	182	396	584	889	1,180	1,500	1,860	2,410
7	241	434	597	839	1,050	1,260	1,500	1,840
7B	109	190	258	373	484	612	759	1,020
7C	101	168	222	310	390	483	584	744
8	356	751	1,150	1,850	2,470	3,260	4,230	5,980
10	227	467	717	1,160	1,560	2,050	2,670	3,820

[1]: rounded to three significant figures

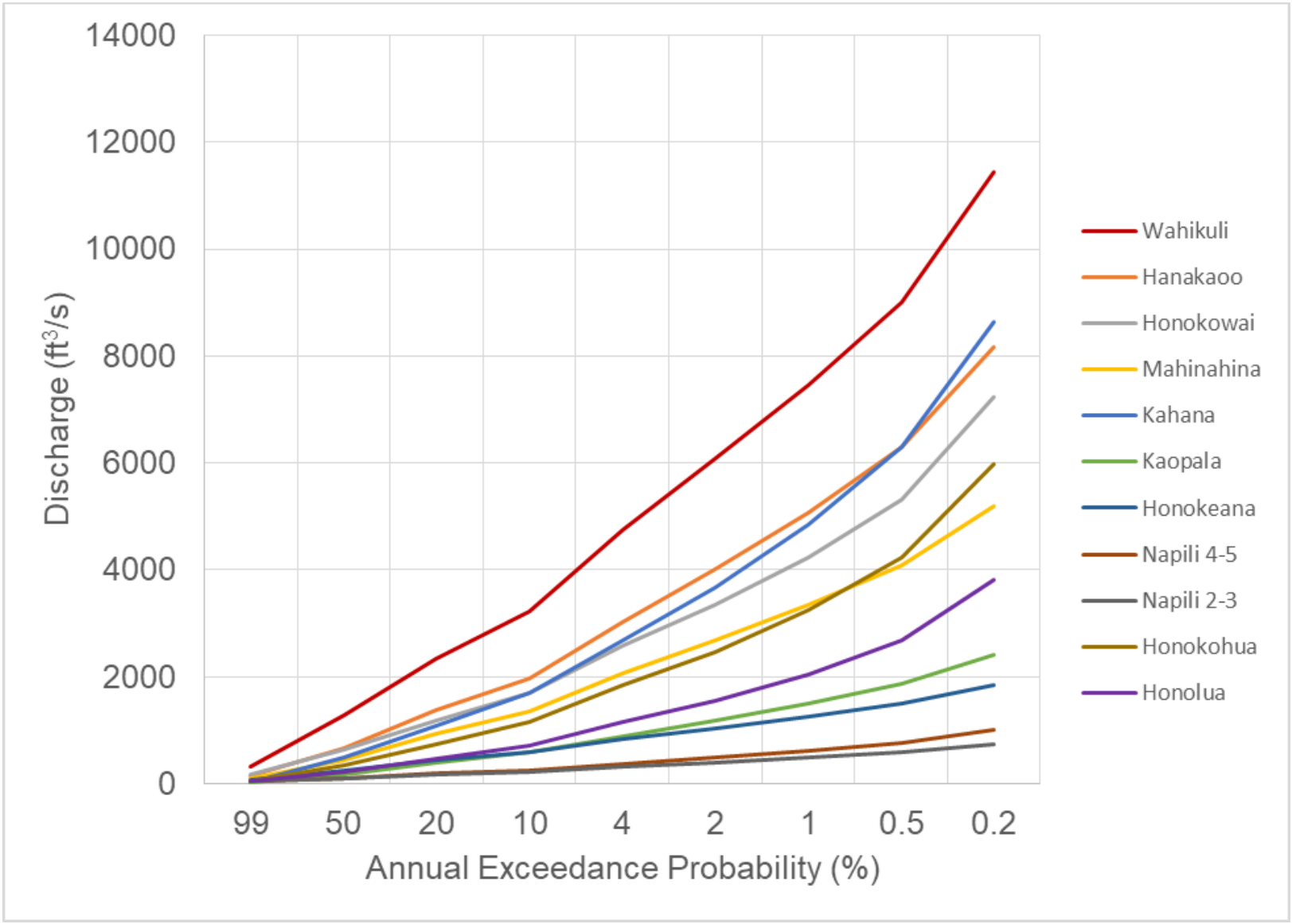

Figure 5-2: Flow Duration Curves for West Maui Basins

Table 5-26: Peak flow estimates for each subbasin

Sub-basin ID	Peak flow (ft^3/s)[1]							
	1/2	1/5	1/10	1/25	1/50	1/100	1/200	1/500
1A	173	297	392	530	639	755	879	1,060
1B	855	1,530	2,100	3,050	3,860	4,680	5,620	7,060
1C	407	787	1,100	1,650	2,150	2,680	3,270	4,200
2A	178	355	503	755	972	1,200	1,460	1,840
2B	515	1,070	1,550	2,390	3,190	4,060	5,040	6,580
3A	198	343	457	621	755	900	1,060	1,290
3B	497	912	1,300	1,930	2,460	3,020	3,660	4,630
3C	177	333	488	764	997	1,270	1,620	2,200
3D	284	562	801	1,170	1,560	2,060	2,650	3,650
4A	453	933	1,360	2,070	2,690	3,340	4,090	5,180
5A	56	95	125	168	204	243	285	344
5B	228	510	763	1,190	1,620	2,090	2,630	3,460
5C	300	657	1,040	1,650	2,250	3,020	4,010	5,620
6A	182	396	584	889	1,180	1,500	1,860	2,410
7A	241	434	597	839	1,050	1,260	1,500	1,840
7B	109	190	258	373	484	612	759	1,020
7C	101	168	222	310	390	483	584	744
8A	203	430	663	1,080	1,440	1,910	2,510	3,600
8B	164	342	524	832	1,100	1,450	1,860	2,560
10A	182	342	486	692	860	1,040	1,240	1,540
10B	140	308	478	797	1,090	1,440	1,910	2,770
10C	142	285	438	696	913	1,190	1,520	2,080
12A	1,780	2,870	3,800	5,250	6,570	8,130	9,860	12,800

[1]: rounded to three significant figures

Table 5-27: Peak flow estimates at key locations

Junction Name	Drainage area (mi^2)	Peak flow (ft^3/s)[1]								
		1/1	1/2	1/5	1/10	1/25	1/50	1/100	1/200	1/500
CWRM 6-124	2.23	56	284	562	801	1,170	1,560	2,060	2,650	3,650
CWRM 6-158	3.89	16	217	458	705	1,150	1,540	2,030	2,640	3,750
Wahikuli Junction	3.65	320	634	1,180	1,690	2,550	3,320	4,190	5,270	7,140
Honokowai Dam	5.56	174	1,260	2,310	3,200	4,690	6,000	7,350	8,880	11,300
Kahana Dam	4.28	62	493	1,090	1,690	2,670	3,650	4,820	6,270	8,600
USGS -0000	4.18	686	1,780	2,870	3,800	5,250	6,570	8,130	9,860	12,800
USGS -0200	5.74	108	461	895	1,290	1,940	2,560	3,330	4,270	5,850

[1]: rounded to three significant figures

5.5 Reference Flows

5.5.1 2015 Flood Insurance Study

In 2015, the Federal Emergency Management Agency (FEMA) published peak flow estimates for various streams in West Maui (FEMA, 2015). These flow estimates are included here:

Table 5-28: Summary of Peak Flow Estimates by FEMA

Flooding Source and Location	Drainage Area (mi^2)	Peak Flow (ft^3/s)			
		1/10	1/50	1/100	1/500
Honokahua Stream at mouth	3.8	1,670	3,360	4,300	7,020
Honokeana Bay Gulch at mouth	0.6	350	670	830	1,300
Honokowai Stream at mouth	6.0	2,000	4,000	5,200	8,200
Kahana Stream at mouth	4.6	2,000	4,000	5,100	8,400
Kahoma Stream at mouth	5.3	2,600	5,100	6,400	10,200
Kaopala Gulch at mouth	0.95	550	1,100	1,300	2,100
Mahinahina Gulch at mouth	1.9	930	1,800	2,300	3,700
Napili Gulch 2-3 at mouth	0.8	420	810	1,020	1,600
Napili Gulch 4-5 at mouth	0.9	540	1,000	1,300	2,000

6 Development of the Hydraulic Model

Two types of hydraulic models were created using the Hydrologic Engineering Center's River Analysis System (HEC-RAS) software (version 6.0.0 Beta 3, HEC, 2021) with the ultimate objective of developing flow and sediment load time series data at five different watershed outlets for various frequency events. The five watersheds selected for detailed modeling are: Honolua, Ka'opala, Kahana, Honokowai, and Wahikuli. These watersheds were selected based on their ability to provide a broad perspective of the varying site conditions across the entire study area (from the northern, wet Honolua watershed to the southern, dry Wahikuli watershed), the availability of corresponding historical stream flow data (Honolua and Honokowai), their estimated annual sediment load (Kahana has the greatest annual sediment load at 285 metric tons per year), and the perceived opportunity for implementation of a proposed management measure.

The first model – a one-dimensional (1D), steady flow hydraulic model – was created to establish an elevation versus discharge rating curve at two sites where stream gages were recently installed in Honolua and Honokowai: CWRM 6-158 and CWRM 6-124, respectively (Section 4.2). A rating curve allows for the stage data collected by the gages to be converted into flow data.

The second model – a two-dimensional (2D), unsteady flow hydraulic model – was created to estimate the amount of sediment eroded from the banks (mass load) over time for various frequency events, specifically along reaches near agricultural fields with historic fill terraces. It does not include considerations of deposition or the effects of any existing or proposed management measures, which were calculated separately.

6.1 Development of the 1D, Steady Flow Model

A simple, steady flow hydraulic model was created to establish a rating curve at two sites where stream gages were recently installed. The rating curve allows for the stage data collected by the gages to be converted into flow data.

Four to five cross sections were surveyed in the field at each site during the time of gage installation (Section 4.2). This data was used to create the geometry for the hydraulic model (Figure 6-1). The model was run using the *mixed* flow regime for Honolua and *supercritical* flow regime for Honokowai under twenty five (25) different flow profiles (0.1 to 20,000 ft^3/s). *Normal depth* was used for the upstream and downstream boundary conditions, which was assumed to be equivalent to the average slope of the channel bed upstream and downstream, respectively. A Manning's roughness coefficient of 0.045 was used for Honolua and 0.050 for Honokowai, reflective of site conditions observed in the field (Photo 6-1 and Photo 6-2).

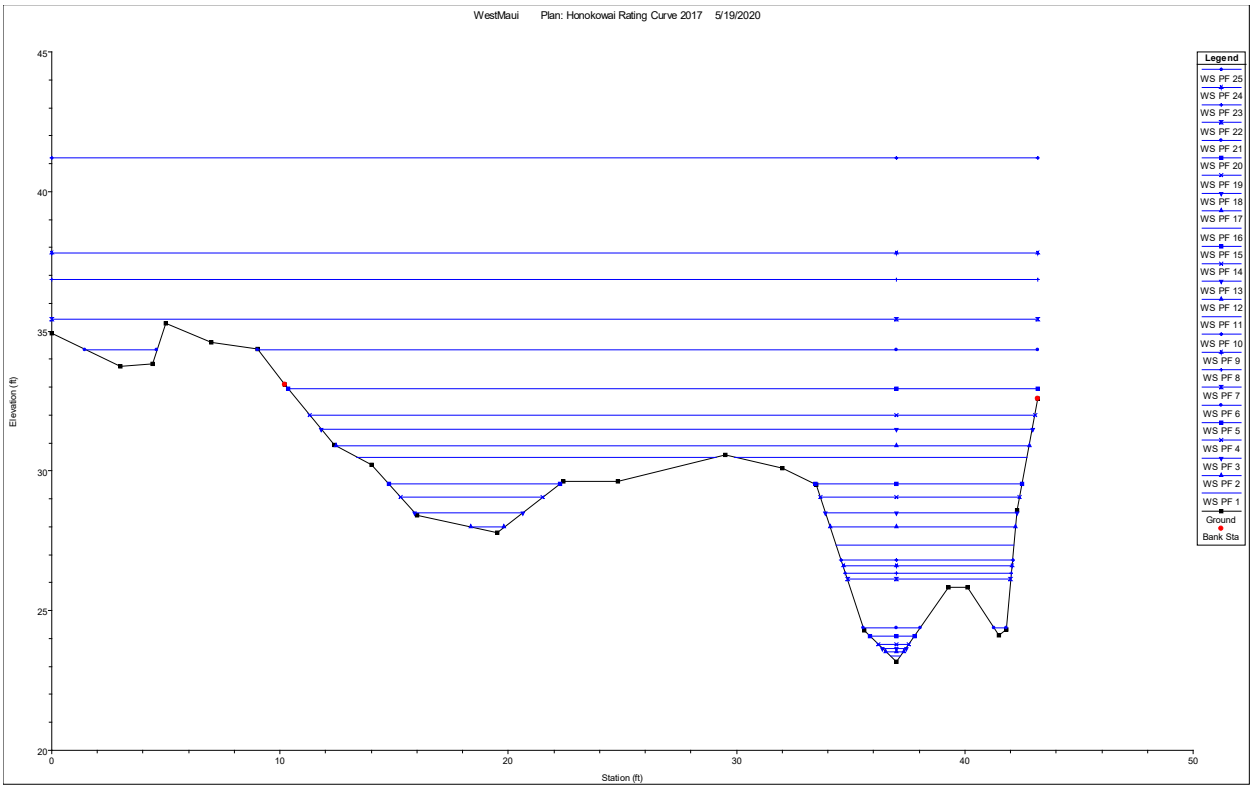

Figure 6-1: HEC-RAS Cross-Section Profile for Honokowai (XS 3)

Photo 6-1: Typical Channel Bed Conditions for Honolua (*n* = 0.045)

Photo 6-2: Typical Channel Bed Conditions for Honokowai (*n* = 0.050)

A rating curve was developed for each site using those flow profiles which provided a positive stage (with reference to the gage datum) and did not exceed the surveyed cross-section profile. The established rating curve for Honolua, which is applicable for recorded stages from 1 – 8 ft and has an R^2 value of 0.9951, is:

$$Q = 61.669H^2 - 116.45H + 66.975$$

where,

Q = flow rate (ft^3/s); and

H = stage (ft)

The established rating curve for Honokowai, which is applicable for recorded stages from 1 – 8 ft, is:

$$Q = 108.77H^2 - 628.32H + 924.63$$

As an example of the application of these equations, the peak flow for two historical events at these sites were estimated and are presented in Table 6-1.

Table 6-1: Peak Flow Estimates for Historical Storm Events

Event	CWRM 6-158 (Honolua)	CWRM 6-124 (Honokowai)
October 24, 2017	1,410 ft^3/s	1,080 ft^3/s
September 12, 2018	3,040 ft^3/s	910 ft^3/s

6.2 Development of the 2D, Unsteady Flow Model

A 2D, unsteady flow hydraulic model was created for the five watersheds previously identified with the objective of acquiring typical flow and shear stress values over time for various frequency events. This data would then be used to estimate sediment flux (mass over time) at critical points in the river system (i.e. the outlet, sited management measures).

6.2.1 **Flow Data**

Peak flow rates determined previously (Section 5.4) were used to represent the amount of water in the system.

6.2.1.1 Boundary Conditions

Boundary conditions are necessary to establish the starting water surface at the upstream and downstream ends of the channel system. A flow hydrograph was used to represent the amount of flow entering at the upstream ends of the hydraulic model. At some locations, it was necessary to further divide the hydrograph developed for each subbasin to represent flow entering from an additional location (typically, a smaller tributary). In this instance, the hydrograph was divided based on the corresponding drainage area for each individual reach segment.

The downstream boundary condition was set to a water surface elevation of 1.13 ft, representing the mean higher high water (MHHW) elevation (in reference to mean sea level) of the ocean. This was determined based on the MHHW elevation at NOAA tidal station at Kahului Harbor, HI – Station ID: 1615680 (NOAA).

A lateral boundary condition was set to normal depth at locations where flow may continue landward (likely north or south) beyond the limits of the model. The normal depth was set to the land slope.

6.2.2 **Geometry Data**

RAS Mapper, a geospatial interface in the HEC-RAS software, was used to fully develop the geometric data required for the river hydraulics model. The projection was set to State Plane Zone 2 (US Survey Feet) with reference to the NAD83 (PA11) coordinate system. Elevation data presented in Section 3.2 were imported to create the

terrain model. Several geometric layers required for the hydraulic model were digitized, some of which are described in Table 6-2.

Table 6-2: GIS layers created for 2D hydraulic models

GIS layer	Description
2D Flow Areas	2D Flow Areas are created by constructing polygon areas representing the regions to be modelled.
Boundary Condition	A Boundary Condition (BC) line was added to identify the location for a specific flow condition on the boundary of a 2D Flow Area.
Breakline	Breaklines were sometimes used in 2D Flow Areas to align the computation cell faces along high ground and natural barriers that affect flow and direction (such as river banks).
SA/2D Area Connection	This internal connection feature can be used to represent embankment crests and major roads.

6.2.3 **Manning's Roughness Coefficient, *n***

Manning's roughness coefficient, *n*, is an empirically derived coefficient that is dependent on several variables, such as vegetation, obstructions, and meandering when applied to open channels. This value was selected based on site characteristics observed in the field, aerial imagery, and geospatial data as provided by the PAC-RISA program (Section 3.5). Typical *n* values selected for this study are provided in Table 6-3 for 2D Flow Areas.

These values and the geospatial data provided by PAC-RISA were used to create a Manning's n layer in RAS Mapper. 2D Flow Areas in the hydraulic model refer to this layer. At some locations, it was necessary to override the default values provided by this layer by identifying a specific area and roughness coefficient. For example, a Manning's n value of 0.045 was assigned to the footprint of the Honolua Stream, overriding default values for forest and shrub areas.

Table 6-3: Manning's n values

Land Cover Type	Manning's *n*
Alien forest, fog	0.16
Alien forest, no fog	0.16
Coffee	0.035
Developed, high-intensity	0.15
Developed, low-intensity	0.1
Developed, medium-intensity	0.08
Developed, open space	0.04
Diversified agriculture	0.035
Fallow/grassland	0.03
Golf course	0.03
Grassland	0.035
Native forest, fog	0.16
Native forest, no fog	0.16
Reservoir, not Iao	0.035
Shrubland	0.1
Sparsely vegetated	0.03
Taro	0.07
Tree plantation, no fog	0.1
Water body	0.035
Wetland	0.07

6.2.4 **Bridges**

Bridges and major culverts were represented in the model as an *SA/2D Area Connection*. Bridge data (e.g. deck width, horizontal span) required for this modeling feature was based on as-built drawings, field measurements, and as provided by *BridgeReports.com*, a searchable version of the National Bridge Inventory (Baughn, 2019). A weir coefficient of 2.6 was selected, representative of flow over a typical bridge deck. At locations where bridge data was not available, the terrain raster was modified to remove these obstacles from the raster completely, allowing for channel flows to pass through unimpeded. Considering the design flood for this study is relatively small (0.5 AEP), bridges are generally not expected to have a significant impact on flows in the channel system.

6.2.5 **Results**

The results of these models provide flow and shear stress time series data, which were used to compute sediment load time series data externally in a spreadsheet (Section 7).

7 Sediment Transport

Sediment transport is a complicated science due to the many variables required to understand the process, such as channel geometry, material density, energy gradient, temperature, viscosity, water turbulence, soil distribution, particle size and shape, soil density, material cohesiveness, and soil concentration. The methodology used for this analysis assumes a simpler approach depended upon the excess shear. The Krone and Partheniades methodology was used. The goal of the sediment transport analysis was to obtain a time series of the sediment load at the end of each reach under existing conditions and two alternatives (an alternative may include one or several sited, proposed management measures across the study area). The process for determining the sediment load at each outlet was in two parts: 1) estimating the total sediment load contributed from riverine sources (bank erosion), and 2) calculating the effectiveness of existing and proposed management measures to capture sediment (deposition). The effectiveness of existing detention basins regarding sediment deposition is discussed in Section 7.2. Proposed management measures are discussed in the following appendix.

7.1 Part 1: Bank Erosion

The general steps for this part of the sediment transport analysis (estimating the total sediment load contributed from riverine sources) are described below:

1. Determine the recurrence of plume-triggering events: with what frequency do sediment plumes occur based on real observation?
2. Determine the total event-based sediment load for a typical plume-triggering event.
3. Using output from the 2D, unsteady flow hydraulic model (i.e. shear stress time series data), compute the sediment load time series data using the excess shear equation by spreadsheet.
4. Determine specific grain size distributions for the sediment load time series data.

7.1.1 **Recurrence of Plume-Triggering Events**

In 2019, the USGS estimated that approximately 3-5 rainfall events typically occur each year that trigger a coastal sediment plume. The triggering event was rainfall with intensities of 10-20 mm/hr (0.4-0.8 in/hr) for at least two hours. This occurred 9 times over the two year period between 2014 and 2016, based on historic records at the West Maui R2R climate stations (Table 4-1). A rainfall frequency analysis at the *Field 46* and *Lahaina* climate stations, representative of the *wet* and *dry* watersheds in the study area, respectively, indicate a recurrence interval of this type of event (two-hour intensities above 10 mm/hr) occurring about three times a year on the *wet side* and about once a year on the *dry side* based on a longer period of record (Stock & Cerovski-Darriau, 2019).

For this study, the recurrence interval of plume-triggering storm events was determined based on precipitation frequency data, as provided by NOAA Atlas 14. Precipitation estimates for a duration of 2 hours at various frequencies were taken at the centroid location of each watershed. These precipitation estimates were plotted on a graph and extrapolated with a logarithmic trendline to determine the approximate frequency for 0.4 in/hr (10 mm/hr) intensities over a 2 hour time period. Recurrence intervals from this type of analysis estimate that plume-triggering storm events occur approximately 2-3 times each year (

Table 7-1).

Table 7-1: Recurrence intervals of plume-triggering storm events

Basin / Subbasin ID	Watershed name	Annual exceedance probability (AEP)	Recurrence interval (yr)
10	Honolua	2.4	0.42
8A	Honokahua	2.2	0.46
8B	Honokahua	2.3	0.44
7A	Honokeana	1.9	0.52
7B	Napili 4-5	2.0	0.50
7C	Napili 2-3	2.0	0.47
6	Ka‘opala	1.9	0.52
5	Kahana	2.0	0.49
4	Mahinahina	1.8	0.55
3	Honokowai	2.9	0.34
2A	Hanakaoo	1.7	0.59
2B	Hanakaoo	2.0	0.49
1	Wahikuli	3.2	0.31

7.1.2 **Annual Load of Sediment**

While one of the objectives of this study is to provide event-based time series data for sediment load at various outlet points in the study area, the total annual load was previously estimated by USGS in 2019 for various source watersheds (Table 7-2). This estimate was based on field surveys of the extent of historic fill terraces and channel geometry along four streams, and two years of bank erosion measurements from four sites. It was also noted that during this two-year period, there were 9 events that exceeded the 10 mm/hr (0.4 in/hr) threshold and likely resulted in a coastal sediment plume. The annual peak flows recorded at USGS -0000 during this period indicate that none of the 9 events were particularly significant and have an approximate flow frequency of 0.5 AEP. For this reason, the 0.5 AEP (2 yr recurrence interval) was selected as the design frequency for establishing baseline conditions and evaluating the effectiveness of proposed mitigation measures. The average load for this type of event was estimated by dividing the total annual load by 4.5.

Table 7-2: Estimate of the annual mass load from bank erosion

USACE Basin / Subbasin ID	USGS Basin ID	Watershed name	Drainage area (km^2)	Estimate of storm mass load from bank erosion (metric tons)	
				Total annual	Plume-triggering event (0.5 AEP)
10	2	Honolua	11.00	91	20.2
8A	9	Honokahua	6.65	45	10.0
8B	8	Honokahua	4.03	46	10.0
7A	16	Honokeana	1.94	43	9.56
7B	14	Napili 4-5	2.41	56	12.4
7C	13	Napili 2-3	1.98	44	9.78
6	20	Ka‘opala	2.36	62	13.8
5	22	Kahana	11.68	285	63.3
4	26	Mahinahina	5.00	45	10.0
3	28	Honokowai	15.20	62	13.8
2A	30	Hanakaoo	5.94	26	5.78
2B	31	Hanakaoo	1.65	25	5.56
1	35	Wahikuli	10.42	42	9.33

7.1.3 **Excess Shear Equation**

The erosion rate of fine-grained soils due to overland flow or stream channel scour is commonly predicted by the excess shear stress equation (Hanson & Cook, 1997):

$$\varepsilon = k_d(\tau_a - \tau_c)^a$$

in which

ε = erosion rate, m/s;

k_d = erodibility coefficient ($m^3/N{\cdot}s$);

a = exponent typically assumed to be 1;

τ_a = applied shear stress on the soil boundary (Pa);

τ_c = critical shear stress (Pa);

Erosion rate, ε, is the mass eroded per unit bed area per unit time. Multiplying this by the area of deposit provides the total sediment load. Estimated bank erosion rates are provided in Table 7-3, calculated by taking the approximate total mass loads for a plume-triggering event (Table 7-2) and dividing it by previously estimated areas of deposit (Stock & Cerovski-Darriau, 2019).

Table 7-3: Surface Area of Terrace Fill Deposit

Watershed name	Impacted Stream Length (m)[1]	Terrace Height (m)[2]	Area of Deposit (m^2)[3]	Erosion Rate, ε (m/s)[4]
Honolua	17,620	1.19	20,968	3.71E-04
Ka‘opala	11,962	1.16	13,876	3.82E-04
Kahana	54,992	1.16	63,791	1.25E-04
Honokowai	33,452	1.13	37,801	2.06E-04
Wahikuli	22,904	1.13	25,882	3.01E-04

[1]: From Table 9 in *Sediment Budget for Watershed of West Maui, Hawai'i*, SIR 2019-xxxx, USGS

[2]: Representative terrace height based on Table 7 in *Sediment Budget for Watershed of West Maui, Hawai'i*, SIR 2019-xxxx, USGS

[3]: Area of deposit = impacted stream length x terrace height

[4]: assumes a bulk density of 1,300 kg/m^3

The erodibility coefficient, k_d, is a measure of the rate of change of erosion resulting from a change in stress above the critical stress. The value of this parameter was selected by calibrating to the erosion rate, ε, presented in Table 7-3..

Table 7-4: Erodibility Coefficient, k_d

Watershed name	River Name	Erosion rate, ε (m/s)[1]
Honolua	Honolua River	4.73E-10
Honolua	Papua Gulch	2.261E-10
Ka'opala	Ka'opala	4.596E-10
Kahana		
Honokowai		
Wahikuli		
[1]: assumes a bulk density of 1,300 kg/m^3		

Excess shear refers to the difference between the applied shear stress, τ_a, and the critical shear stress, τ_c. A time series of the average shear stress applied to soil boundary (the channel's bed and banks), τ_a, was determined based on the computed outputs by the hydraulic model (Section 7.1.4). Critical shear stress, τ_c, is the shear stress required to initiate erosion. In 2017, USGS performed a cohesive strength meter (CSM) test to quantify the *in situ* erosion resistance of the fill terrace sediments. The critical erosion threshold was defined as the pressure step at which transmission dropped below 90%. This process often involves both shear and normal stresses. An empirical calibration was developed for the CSM by Grawbowski et al. (2010) by comparing erosion thresholds generated in the CSM and annular flume using homogenous sand and mud mixtures. For stagnation pressures, P_{stag}, ranging from 30 to 110 PA, critical shear stress was estimated by the following equation:

$$\tau_c = 0.0013 P_{stag} + 0.047$$

While stagnation pressures measured in West Maui were above this threshold, this empirical equation was still considered to be the most appropriate method for estimating critical shear stress at each site. The average critical shear stress calculated for wet and dry watershed sites were very similar, 0.87 and 0.86, respectively (Table 7-5). A critical shear stress of 0.865 was selected as the representative value for all watersheds.

Table 7-5: Estimates of critical shear stress

Location	Stagnation pressure, P_{stag}, at 90% transmission (Pa)	Critical shear stress, τ_c (Pa)
Southern, "dry" watersheds		
Wahikuli Stream	300	0.44
Honokowai Stream	400	0.57
Mahinahina Gulch	1,200	1.6
	Average	**0.87**
Honolua Stream	200	0.31
Lower Papua Gulch	700	0.96
Upper Papua Gulch	1,000	1.3
	Average	**0.86**

7.1.4 Hydraulic Model Data

In the current version of HEC-RAS (ver. 6.0.0 Beta 3), flow and shear stress time series data can be computed for each cell face. Data was collected from several cell faces that were within the main channel (a minimum of 5 per reach being evaluated; at least 300 ft apart; and more than 50% inundated during the simulation). This data was used, with the excess shear equation (Section 7.1.3), to compute sediment load time series data externally in a spreadsheet using Microsoft Excel software.

7.1.4.1 Key Assumptions and Limitations

It is assumed that once the sediment is lifted, it does not settle as it travels to the stream outlet unless it comes across an obvious management feature (either existing or proposed). The 2D, unsteady flow hydraulic model does not account for the fall or settling velocity of the material, or any flocculation occurring within the reach. Deposition by specific management measures were calculated separately (Section 7.2).

Another assumption of this model is that only the fill terraces are providing the sediment load. This assumption was made due to the understanding that the fill terraces are the primary cause of plumes within the ocean (USGS, 2019).

It was assumed that the 0.5 AEP would provide 4.5 times of the annual fine sediment load as documented within the sedimentation budget (USGS, 2019). Then, this

amount of sediment was matched to the computed flux to understand the uncertainty in the critical shear and erodibility factor of the soil. Additionally, this is a static sedimentation transport model based on an unsteady flow, so it does not capture any backwater conditions that would cause sediment deposition

This model depends only upon the critical shear and does not take into consideration the many other variables that affect soil transport. Therefore, it should only be used to compare alternatives that could impact flow, water depth, and/or shear stress, since shear stress is a function of water depth.

There is variability within the critical shear and erodibility factors, and these factors cause the results to be sensitive. These factors were modified to solve and calibrate the model for when plumes have occurred as reported by USGS studies.

An example figure of the flow and flux time series data computed is provided as Figure 7-1.

7.1.5 **Grain Size Distribution**

Without turbidity samples to use for calibration, it was assumed that the grain size distribution of the sediment load in transport was comparable to the grain size distribution of the cohesive fill terrace sediment samples collected by USGS (Table 4-7). An example figure of sediment distribution is provided as Figure 7-2.

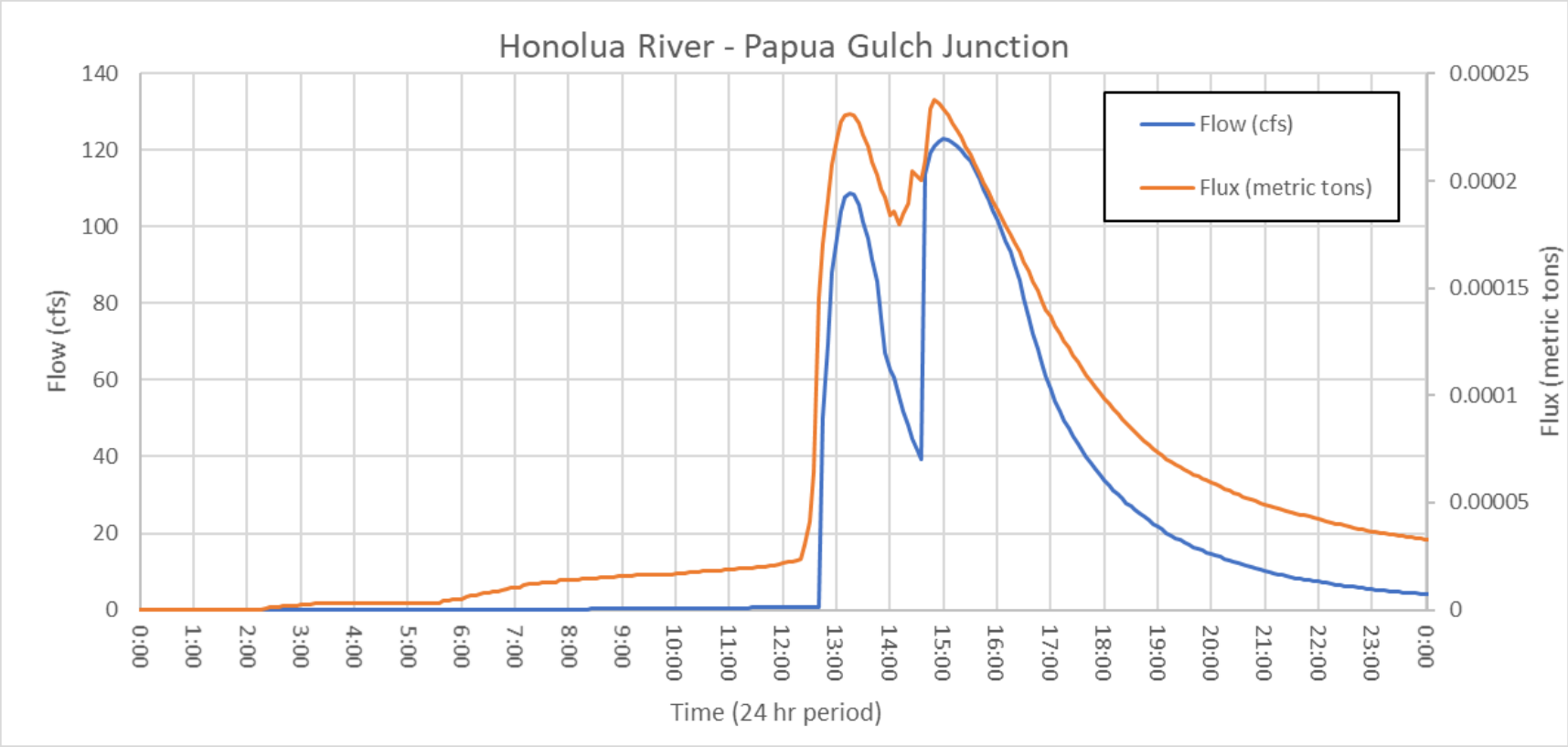

Figure 7-1: Flow and Flux Time Series Data for the Honolua River – Papua Gulch Junction, Honolua Watershed, 0.5 AEP (2-year) Flood

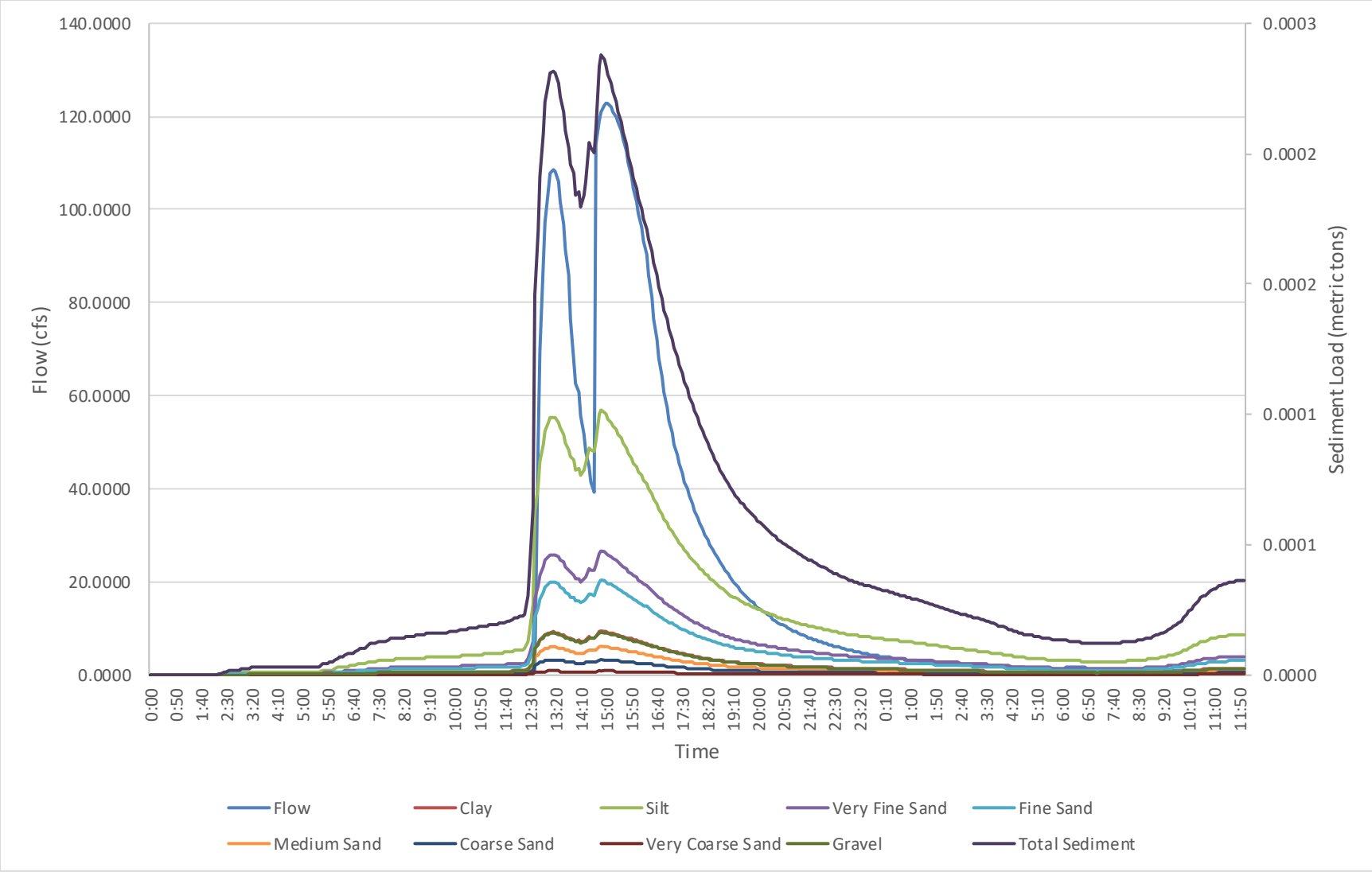

Figure 7-2: Sediment Distribution for the Honolua River – Papua Gulch Junction, Honolua Watershed, 0.5 AEP (2-year) Flood

7.2 Part 2: Sediment Deposition

The annual sediment load that was estimated by USGS in 2019 for each watershed was based on maintenance records of the amount of sediment removed across the various detention basins. Therefore, the estimated load does not include consideration of the effectiveness of these detention basins. Of the five watersheds being closely evaluated in this study, three watersheds have detention basins: Kaopala, Kahana, and Honokowai. The trap efficiency of each basin to retain sediment during a specific type of flood event (e.g .the 0.50 AEP flood) was estimated using Camp's [1946] settling velocity equations, which are as follows:

$$TE = \frac{vA}{Q}$$

where TE = trap efficiency

V = settling velocity (ft/s)

A = wetted surface area (ft^2)

Q = discharge rate (ft^3/s)

The settling velocity of clay, silt, and fine sand in stormwater can be estimated using Stoke's Law, given in the equation below:

$$V_s = \frac{g\left(\frac{p_1}{p} - 1\right)d^2}{18\upsilon}$$

where:

V_s = settling velocity of the solid

g = acceleration of gravity

$p1$ = mass density of the solid

p = mass density of the fluid

d = diameter of the solid (assuming spherical)

υ = kinematic viscosity of the fluid

For particles larger than fine sand, such as coarse gravel, the equation by Ferguson and Church is used:

$$V_s = \frac{gRd^2}{18\upsilon + (0.75CgRd^3)^{1/2}}$$

where:

V_s = settling velocity of the solid

g = acceleration of gravity

d = diameter of the solid (assuming spherical)

R = specific gravity of the particle in water

C = a constant equal to 0.4 for spheres and 1 for typical sand grains

The assumed values for each parameter needed for either equation are listed in Table 7-6. Based on average diameter limits for various soil types, typical settling velocities are provided in Table 7-7.

Table 7-6: Assumed Parameter Values for Settling Velocity Equations

Parameter	Value[1]
g	9.81 m/s^2
p1	2650 kg/m^3
p	998 kg/m^3
υ	1.004E-6 m^2/s
R	2.66
C	0.4

[1]: assuming water temperatures of 20 ºC (68 ºF)

Table 7-7: Typical Settling Velocities Based on Soil Type

Name of soil separate	Diameter limits (mm)	Equation	Settling velocity, V_s (m/s)	Settling velocity, V_s (ft/s)
Clay	< 0.002	Stoke's Law	8.99E-07	2.95E-06
Silt	0.002 – 0.05	Stoke's Law	6.07E-04	0.002
Very fine sand	0.05 – 0.10	Stoke's Law	5.05E-03	0.017
Fine sand	0.10 – 0.25	Stoke's Law	2.75E-02	0.090
Medium sand	0.25 – 0.50	Ferguson and Church	0.203	0.666
Coarse sand	0.50 – 1.00	Ferguson and Church	0.812	2.66
Very coarse sand	1.00 – 2.00	Ferguson and Church	3.25	10.7

The wetted surface area and discharge rate parameters are based on the hydraulic model simulation results (Section 6.2). Measurements for the wetted surface area were taken in RAS mapper by drawing a polygon around the inundated basin. Maximum flow across the SA/2D Area Connection is automatically computed, which represents the maximum discharge rate across the spillway or via the underground outlet pipe and was used as the discharge rate in Camp's settling velocity equations (

Table 7-8). The trap efficiency of each basin (Table 7-9: Discharge Rates for the 0.50 AEP Flood Event for the Kaopala, Kahana, and Honokowai Basins

Basin	Discharge, Q_{out} (ft^3/s)	
	Outlet	Spillway
Kaopala	9.37	3.94[1]
Kahana		
Honokowai	306	0
[1]: The Kaopala spillway was just barely activated by the 0.50 AEP flood		

Table 7-10: Volumes of Water for the 0.50 AEP Flood Event for the Kaopala, Kahana, and Honokowai Basins

Basin	Volume (ft^3)		
	Reservoir invert to outlet pipe	Outlet pipe to spillway	Above spillway
Kaopala	65,599	487,709	70,036
Kahana			
Honokowai	0	9,343,606	0

Table 7-11 to Table 7-13) was applied to the incoming sediment load distribution initially estimated to determine the final sediment load distribution at the outlet.

Table 7-8: Wetted Surface Areas for the 0.50 AEP Flood Event for the Kaopala, Kahana, and Honokowai Basins

Basin	Surface Area, SA (ft^2)		
	at Outlet	at Spillway	Maximum
Kaopala	22,241	48,423	48,423
Kahana			
Honokowai	--	--	235,300

Table 7-9: Discharge Rates for the 0.50 AEP Flood Event for the Kaopala, Kahana, and Honokowai Basins

Basin	Discharge, Q_{out} (ft^3/s)	
	Outlet	Spillway
Kaopala	9.37	3.94[1]
Kahana		
Honokowai	306	0
[1]: The Kaopala spillway was just barely activated by the 0.50 AEP flood		

Table 7-10: Volumes of Water for the 0.50 AEP Flood Event for the Kaopala, Kahana, and Honokowai Basins

Basin	Volume (ft^3)		
	Reservoir invert to outlet pipe	Outlet pipe to spillway	Above spillway
Kaopala	65,599	487,709	70,036
Kahana			
Honokowai	0	9,343,606	0

Table 7-11: Trap Efficiency for Various Soil Types, Kaopala Basin, 0.50 AEP Flood

Name of soil separate	Diameter limits (mm)	Trap Efficiency (%)
Clay	< 0.002	1.60
Silt	0.002 – 0.05	> 100
Very fine sand	0.05 – 0.10	> 100
Fine sand	0.10 – 0.25	> 100
Medium sand	0.25 – 0.50	> 100
Coarse sand	0.50 – 1.00	> 100
Very coarse sand	1.00 – 2.00	> 100

Table 7-12: Trap Efficiency for Various Soil Types, Kahana Basin, 0.50 AEP Flood

Name of soil separate	Diameter limits (mm)	Trap Efficiency (%)
Clay	< 0.002	
Silt	0.002 – 0.05	> 100
Very fine sand	0.05 – 0.10	> 100
Fine sand	0.10 – 0.25	> 100
Medium sand	0.25 – 0.50	> 100
Coarse sand	0.50 – 1.00	> 100
Very coarse sand	1.00 – 2.00	> 100

Table 7-13: Trap Efficiency for Various Soil Types, Honokowai Basin, 0.50 AEP Flood

Name of soil separate	Diameter limits (mm)	Trap Efficiency (%)
Clay	< 0.002	0.23
Silt	0.002 – 0.05	> 100
Very fine sand	0.05 – 0.10	> 100
Fine sand	0.10 – 0.25	> 100
Medium sand	0.25 – 0.50	> 100
Coarse sand	0.50 – 1.00	> 100
Very coarse sand	1.00 – 2.00	> 100

8 Conclusion

The final event-based sediment load and distribution time series data at the outlet of five key watersheds within the study area were determined by flood frequency analysis, use of hydraulic modeling, calibration of event-based sediment loads to previous investigations, and analysis of the trap efficiency of existing detention basins. The five watersheds selected for this type of analysis were Wahikuli, Honokowai, Kahana, Kaopala, and Honolua. Peak flow estimates were developed for all eleven watersheds within the study area: Wahikuli, Hanakaoo, Honokowai, Mahinahina, Kahana, Kaopala, Honokeana, Napili 4-5, Napili 2-3, Honokohua, and Honolua.

The flood frequency analysis included stream gage analysis, application of regional regression equations, and development of a rainfall-runoff model using HEC-HMS software. The rainfall-runoff model was initially calibrated to replicate specific historical storms; however, the limited number of sites and storm events that could be used for calibration proved this method to be ineffectual. However, a Bulletin 17C stream gage analysis on two sites in the Honokohau and Honokowai watershed provided a strong level of confidence based on long periods of record and the rainfall-runoff model was calibrated to match these results. The final peak flow estimates adopted by this study are presented in Section 5.4.

The output of the calibrated rainfall-runoff model was used as input for the two-dimensional, unsteady flow hydraulic model that was developed using HEC-RAS software. Models were created that are representative of the lower reaches within the Wahikuli, Honokowai, Kahana, Kaopala, and Honolua watersheds. Flow and shear stress time series data (outputs from the hydraulic model) were then used to develop time series data representative of the likely sediment load within the reach and at the outlet.

The sediment load time series data was developed using the *excess shear* equation, in addition to relying upon previous conclusions drawn by USGS regarding the annual sediment load for each watershed, the types of event that trigger a sediment plume at the outlet, and data collected in the field throughout the study.

The effectiveness of the existing detention basins at Kaopala, Kahana, and Honokowai were determined by using Camp's settling velocity equations. The sediment

load time series data was then adjusted to determine the probable sediment load that was released into the ocean based on existing site conditions. These results are presented in Section 7.2. The level of accuracy of these results is commensurate with the level of data that was available during this study.

9 References

Babcock, R. J., Bteni, S., Francis, O., Falinski, K., Nielson, J., Harada, B., . . . Li, Y. (n.d.).

Baughn, J. (2019). Retrieved from BridgeReports.com: http://bridgereports.com/hi/

Brewington, L. (2018). Maui Future Land Cover Scenarios Version 1.1. Honolulu, Hawaii, USA. Retrieved from Pacific Risa: https://www.pacificrisa.org/projects/maui-groundwater-project/building-the-scenarios/

CASQA. (2010). *California Stormwater BMP Handbook.* California Stormwater Quality Association (CASQA). Retrieved from http://www.stancounty.com/publicworks/pdf/Development/NPDES/SE-02.pdf

CWRM. (2019, June). *Instream Flow Standard Assessment Report, Island of Maui, Hydrologic Unit 6010, Honokowai.* State of Hawaii, Department of Land and Natural Resources. Commission on Water Resource Management (CWRM). Retrieved from https://dlnr.hawaii.gov/cwrm/surfacewater/ifs/westmaui3/

CWRM. (2019). *Instream Flow Standard Assessment Report, Island of Maui, Hydrologic Unit 6013, Honolua.* State of Hawaii, Department of Land and Natural Resources. Honolulu, Hawaii: Commission on Water Resource Management (CWRM). Retrieved from https://dlnr.hawaii.gov/cwrm/surfacewater/ifs/westmaui3/

Daly, E. R., Fox, G. A., Al-Madhhachi, A. T., & Miller, R. B. (2013). *A Scour Depth Approach for Deriving Erodibility Parameters from Jet Erosion Tests.* American Society of Agricultural and Biological Engineers. doi:10.13031

Dober. (n.d.). *Dual Polymer System*. Retrieved from HaloKlear Natural Flocculants: https://www.dober.com/haloklear/dual-polymer-system

FEMA. (2015). *Flood Insurance Study, Maui County, Hawaii.* Federal Emergency Management Agency. Retrieved from https://map1.msc.fema.gov/data/15/S/PDF/150003V001D.pdf?LOC=a97cb530b1a73b07846aade6d004108b

Gingerich, S. B., Yeung, C. W., Ibarra, T.-J. N., & Engott, J. A. (2007). *Water Use in Wetland Kalo Cultivation in Hawaii.* U.S. Department of the Interior. Reston, VA: U.S. Geological Survey (USGS). Retrieved from https://pubs.usgs.gov/of/2007/1157/of2007-1157.pdf

Grabowski, R. C., Droppo, I. G., & Wharton, G. (2010). Estimation of critical shear stress from cohesive strength meter-derived erosion thresholds. *Limnology and Oceanography: Methods*, 678-685. Retrieved from https://aslopubs.onlinelibrary.wiley.com/doi/pdf/10.4319/lom.2010.8.0678

Gregory, R. (2014, August). USA - Hawaii - Restoring the Life of the Land: Taro Patches in Hawai'i. Retrieved from http://ecotippingpoints.org/our-stories/indepth/usa-hawaii-taro-agriculture.html

Hanson, G. J., & Cook, K. R. (1997). Development of Excess Shear Stress Parameters for Circular Jet Testing. *ASAE Annual International Meeting.* Minneapolis Convention Center: ASAE. Retrieved from https://www.bae.ksu.edu/watershed/other/jetworkshop/Hanson%20and%20Cook%201997.pdf

Honolulu Weather Forecast Office. (2020). *Observed Weather: Monthly Weather Summary (CLM)*. (National Oceanic and Atmospheric Administration (NOAA), National Weather Service (NWS), Honolulu Weather Forecast Office) Retrieved from Weather.gov: https://w2.weather.gov/climate/index.php?wfo=hnl

Interagency Advisory Committe on Water Data. (1982). *Flood Flow Frequency.* Reston, VA: U.S. Department of the Interior, Geological Survey, Office of Water Data Coordination. Retrieved from https://water.usgs.gov/osw/bulletin17b/dl_flow.pdf

Mishan, L. (2019, November 8). On Hawaii, the Fight for Taro's Revival. *The New York Times Style Magazine*. The New York Times Style Magazine. Retrieved from https://www.nytimes.com/2019/11/08/t-magazine/hawaii-taro.html

Moriasi, D. N., Arnold, J. G., Van Liew, M. W., Bingner, R. L., Harmel, R. D., & Veith, T. L. (2007). *Model evaluation guidelines for systematic quantification of accuracy in watershed simulations.*

MRLC. (2011). *Data*. Retrieved from Multi-Resolution Land Characteristics Consortium: https://www.mrlc.gov/data

Napili Bay and Beach Foundation. (n.d.). *Napili 4-5 Desilting Basin*. Retrieved from Napili Bay and Beach Foundation: https://napilibayfoundation.org/napili-4-5-desilting-basin/

NCEI. (n.d.). *Climate Data Online*. Retrieved from National Centers for Envrionmental Information: https://www.ncdc.noaa.gov/cdo-web/

NOAA. (2017, April 21). *NOAA Atlas 14 Point Precipitation Freqeuncy Estimates*. (National Oceanic and Atmospheric Administration. National Weather Service. Hydrometeorological Design Studies Center) Retrieved from Precipitation Frequency Data Server (PFDS): https://hdsc.nws.noaa.gov/hdsc/pfds/pfds_map_hi.html

NOAA. (n.d.). *Datums for 1615680, Kahului, Kahului Harbor HI*. Retrieved from Tides & Currents: https://tidesandcurrents.noaa.gov/datums.html?id=1615680

NRCS. (n.d.). (United States Department of Agriculture, Natural Resources Conservation Service (NRCS)) Retrieved from Web Soil Survey: https://websoilsurvey.nrcs.usda.gov/app/

NRCS. (1986). *Urban Hydrology for Small Watersheds*. Conservation Engineering Division. U.S. Department of Agriculture, Natural Resources Conservation Service (NRCS). Retrieved from https://storymaps.arcgis.com/stories/67f74f370af6414f9238e8d61158fd5c

NRCS. (2007). *National Engineering Handbook, Part 630 Hydrology.* United States Department of Agriculture, Natural Resources Conservation Service. Retrieved from https://directives.sc.egov.usda.gov/OpenNonWebContent.aspx?content=17755.wba

NRCS. (2011). *Napili 4-5 Sediment Basin - Application for Removal of Facility from State of Hawaii Jurisdiction.* Natural Resources Conservation Service.

NWS. (2005, October 12). *Unit Hydrograph (UHG) technical Manual*. (National Weather Service - Office of Hydrology, Hydrologic Research Laboratory & National Operational Hydrologic Remote Sensing Center) Retrieved from National Operational Hydrologic Remote Sensing Center: https://www.nohrsc.noaa.gov/technology/gis/uhg_manual.html

Oki, D. S., Rosa, S. N., & Yeung, C. W. (2010). *Flood-Frequency Estimates for Streams on Kaua'i, O'ahu, Moloka'i, Maui, and Hawai'i, State of Hawai'i.* U.S. Department

of the Interior, U.S. Geological Survey. Retrieved from https://pubs.usgs.gov/sir/2010/5035/sir2010-5035_text.pdf

Risk, M. J., & Edinger, E. (2011). *Impacts of Sediment on Coral Reefs.* Durham, ON, Canada.

SCS. (1982). *Honokowai Dam, Structure No. 8.* Honolulu, HI: U.S. Department of Agriculture, Soil Conservation Service (SCS).

State of Hawaii, Office of Planning. (n.d.). Hawaii Lidar Data Download. Retrieved from https://www.arcgis.com/apps/webappviewer/index.html?id=7c22201923084f749e6626e3e195de71

Stock, J. D., & Cerovski-Darriau, C. (2019). *Sediment Budget for Watersheds of West Maui, Hawai'i.* Reston, VA: U.S. Department of the Interior, U.S. Geological Survey.

Storlazzi, C. D., Norris, B. K., & Rosenberger, K. J. (2015, September). The influence of grain size, grain color, and suspended-sediment concentration on light attenuation: Why fine-grained terrestrial sediment is bad for coral reef ecosystems. *Coral Reefs, 34*(3). doi:10.1007/s00338-015-1268-0

University of Hawai'i. (2014). Hawaii Soil Atlas. Hawaii, USA. Retrieved from https://gis.ctahr.hawaii.edu/SoilAtlas

USGS. (n.d.). The National Map. U.S. Geological Survey. Retrieved from https://viewer.nationalmap.gov/basic/

Weber, M., Lott, C., & Fabricius, K. E. (2006). Sedimentation stress in a scleractinian coral exposed to terrestrial and marine sediments with contrasting physical, organic and geochemical properties. *Experimental Marine Biology and Ecology*.